CLUSTER ONE

ENVIRONMENTAL SCIENCE AND HEALTH

Red is the color of blood, symbolizing our deeper connection to our environment and planet. The gem is in the shape of a drop of blood for the same reason. As such, if we are to keep living on this earth, we have to keep track of the environment's status and find ways to solve environmental problems. One of the biggest aims of environmental science is to find solutions to such problems. The striking color of red therefore also inspires and motivates us to take action and work towards this aim.

These studies tackle varying environmental issues. As such, they can be associated with one of the following agendas: the Aquatic, Agriculture, and Natural Resources (AANR) Research and Development Agenda, and the Disaster Risk Reduction and Climate Change Adaptation (DRR & CCA) Research and Development Agenda. This is because the studies are generally aligned with the objectives of the former agenda, while one study has objectives and has aspects more related to the priorities of the latter agenda.

BASED ON: Harmonized National Research and Development Agenda (HNRDA)

Publiscience Vol. 4 Issue 1

Climatological analysis of the Southwest Monsoon (Habagat) in Type 1 Climate Areas in the Philippines from 1949–2018

POLINA S. ESPINO, ALYSA MARIE M. ONG, DANIELLE MARI J. YORAC, and JULNAFE B. LIBO-ON

Philippine Science High School Western Visayas Campus - Department of Science and Technology (DOST-PSHSWVC), Brgy. Bito-on, Jaro, Iloilo City 5000, Philippines

Article Info

Submitted: May 10, 2021
Approved: Aug 11, 2021
Published: Aug 30, 2021

Keywords:
southwest monsoon
habagat
rainfall
climatological analysis
precipitation

Abstract

The Southwest monsoon (SWM) rainfall is used in agriculture, industry, and electrical energy and fills reservoirs that supply water to households. However, it generates high levels of rainfall which can negatively affect Philippine agriculture. The historical behavior and trends of the SWM rainfall in the Philippines were identified using collected rainfall data from fourteen (14) meteorological stations situated in Type 1 climate areas of the country, where the impact of SWM is well-pronounced. The time series analysis from 1949 to 2018 for the months of June to September showed an overall increase in accumulated rainfall with a slope of +1.8047, as well as in the decadal frequencies of high precipitation event days (HPE) at the 85th, 95th, and 99th percentile with slopes of +1.0586, +0.4740, and +0.1030, respectively. The trendline for the no-rain days graph has a slope of -0.1177, indicating a decreasing trend. These findings suggest a possibility of an increase in SWM rainfall in the coming decades.

Introduction. - Heavy rainfall is considered one of the most disastrous weather extremes that greatly affect human activities and environmental systems [1]. The factors that facilitate heavy rainfall events include (i) the southward expansion of the high-pressure system to the north of the Philippines, (ii) the El Niño Southern Oscillation (ENSO), and (iii) enhanced moisture-converged cold surges [2]

The Southwest monsoon (SWM) are trade winds that bring warm and considerably humid air mass during the months of June to September every year. The Southwest monsoon (SWM) rainfall results from the passing of air over large areas of warm equatorial ocean that stimulates evaporation from its surface; as the moisture-heavy air cools, it moves north and precipitates [3]. It contributes 43% of the precipitation in the mean annual rainfall in the Philippines [4]. According to [5], the western side of the country is greatly affected by rainfall from the Southwest monsoon (SWM) during boreal summer. It also simultaneously occurs with the peak occurrence of tropical cyclones in the country which is during the months of July and August. This co-occurrence allows tropical cyclones to influence the southwesterly winds of the monsoon which contributes to an increase in the amount of precipitation during the season [4,6]. Crost et al. [7] found that an increase in rainfall during the dry season increases agricultural production, while rainfall during the wet season harms crops and produces conflict. According to the International Rice Research Institute [8], 30% of the total rice area in the country is rainfed and upland, which are heavily reliant on rainfall for crop production. However, this agricultural system is also sensitive to the variability in rainfall patterns which could bring sudden heavy rainfalls that are damaging to the crops [9]. In 2016, it was found that there is an increasing trend in economic loss and damage due to tropical cyclones [10]. Since the country is vulnerable to variations in climate and rainfall, changes in the onset and intensity of rainfall can significantly affect livelihood, food security, and economic stability, by disrupting agricultural production and damaging infrastructure [5,11].

The East Asian Monsoon and South China Sea Monsoon rainfall trends have been studied intensively over the past years [12,13,14]. However, the rainfall trends of the Southwest monsoon have received relatively little interest from the scientific community, thus the need for this research. The study of Cruz et al. [5] presented data regarding the climatological analysis of Philippine Southwest monsoon rainfall. Their examination of the rainfall extremes indicated an increasing trend in the number of days without rain and a decreasing trend in the heavy rainfall days from 1961 to 2010, which can be detected with statistical confidence. However, multiple meteorological stations have been constructed in other parts of the country since then. A shift in rainfall was also observed in different portions of the country due to the reduction of the topography of mountains, urbanization, and climate change. Hence, utilizing a wider scope of data in terms of geography and time will increase the accuracy of *Habagat* rainfall trends and patterns, thus the need for this study [15].

This observational study analyzed the trend and behavior of SWM or habagat rainfall in the

How to cite this article:
CSE: Espino PS, Ong AMM, Yorac DMJ. 2021. Climatological analysis of the Southwest Monsoon (Habagat) in Type 1 Climate Areas in the Philippines from 1949–2018. Publiscience. 4(1): 2–7.
APA: Espino, P.S., Ong, A.M.M., & Yorac, D.M.J. (2021). Climatological analysis of the Southwest Monsoon (Habagat) in Type 1 Climate Areas in the Philippines from 1949–2018. *Publiscience*, *4*(1), 2–7.

For supplementary data, contact: publiscience@wvc.pshs.edu.ph.

northwestern portion of the Philippines using rainfall data from fourteen (14) synoptic stations from 1949 to 2018. It specifically aims to:

(i) identify the high precipitation event days (HPE) where the total amount of rainfall collected in each station belongs to the upper 85th, 95th, and 99th percentile;

(ii) determine the number of days with and without rain;

(iii) present a time series analysis that will show the trend of rainfall for the past seventy (70) years in the Type 1 climate areas of the Philippines where the impact of SWM is well pronounced;

(iv) identify years where the SWM rainfall deviates from the climate mean;

(v) detect years with normal, below-normal, and above-normal rainfall using the Southwest Monsoon Rainfall Anomaly Index (SWMRAI) threshold; and

(vi) analyze the graphs and investigate the trends present in the graphs.

Methods. - The methodology used for this study was adapted from the study of Cruz et al. [5]. Total rainfall data from the years 1949–2018, collected from fourteen (14) synoptic meteorological stations—the Baguio PAGASA weather station, and thirteen (13) stations which are included in the Climate Type I of the modified Corona's climate classification—were requested from PAGASA. A time-series analysis was used to determine the historical trend and variability of the SWM rainfall. The no-rain days and high precipitation event (HPE) days were then determined and the HPE days were classified into 85th, 95th, and 99th percentiles. Using the calculated spatial average of each standardized rainfall anomaly, the Southwest monsoon Rainfall Anomaly Index (SWMRAI) for each year was obtained. Finally, using the standard deviation of the SWMRAI as the threshold, the SWM rainfall extremes were determined.

Collection of Raw Rainfall Data. The daily, monthly, and annual rainfall data that was used to determine the trends and historical behavior of the Southwest monsoon (SWM) or *Habagat* in the country are from the year 1949 to 2018. They were collected from PAGASA's fourteen (14) synoptic meteorological stations (see Table 1). In this study, the reference period for the baseline climate is from 1949 to 2018. Since the synoptic meteorological stations were not built in the same years, the months with missing data were replaced with the climatological mean of the monthly total rainfall, following the methods of Cruz et al. [5].

Table 1. Coordinates and year built of the fourteen (14) synoptic stations used to determine trends and historical behavior of the southwest monsoon in the country.

Location	Year and Month Built
Ambulong, Batangas	Jan 1951
Baguio City, Benguet	Jan 1949
Cabanatuan, Nueva Ecija	Jan 1989
Coron, Palawan	Jan 1951
Cuyo, Palawan	Jan 1951
Dagupan City, Pangasinan	Jan 1951
Iba, Zambales	Jan 1951
Laoag City, Ilocos Norte	Jan 1951
NAIA (MIA), Pasay City	Jan 1949
Port Area (MCO), Manila	Jan 1949
Puerto Princesa, Palawan	Jan 1951
San Jose, Occ. Mindoro	Jan 1981
Sangley Point, Cavite	Jan 1974
Science Garden, Quezon City	Apr 1961

Data Analysis. The time-series analysis was used to determine the historical trend and variability of the SWM rainfall. From the data provided by PAGASA, days with no rain and HPE were determined. The HPE days were then classified into 85th, 95th, and 99th percentiles, which according to Bagtasa et al. [16], are considered days with heavy rain. Using the formula adapted from Wilks [12], standardized anomalies were determined for each station per year. The Southwest monsoon Rainfall Anomaly Index (SWMRAI) for each year was then obtained using the calculated spatial average of each standardized rainfall anomaly. The standard deviation of the SWMRAI was derived and used as a threshold to determine the rainfall levels.

No-rain Days. The number of days where the rainfall collected in a station is 0 mm was determined per year and tallied per decade. A bar graph was then generated with the decadal frequencies of no-rain days for the months of June to September from 1949 to 2018 for each station.

High Precipitation Events Days. The high precipitation events (HPE) days, days with rainfall in the upper 85th, 95th, and 99th percentile, were determined using daily rainfall data from all fourteen (14) synoptic stations and were tallied per decade. They are referred to as HPE85, HPE95, and HPE99, respectively. A graph containing the decadal frequencies of HPE85 days per station was generated. The same was done for HPE95 and HPE99 days.

Standardized anomalies. A rainfall index was used to determine the annual variation of SWM rainfall per station. Rainfall data from PAGASA is expressed as a standardized anomaly so that it can be directly compared to rainfall data from different stations regardless of local conditions such as elevation and land use. Adapted from Wilks [17], the standardized anomalies are expressed as:

$$(1) \quad Z_i = \frac{x_i - \bar{x}_i}{s_{xi}}$$

Where:

x_i = SWM rainfall value at station i for a particular year
$\bar{x_i}$ = mean SWM rainfall for station i
s_{xi} = standard deviation at station i from 1949–2018

The data that were obtained from this step are 843 Z_i values – one value for each of the fourteen stations per year. The Z_i values were grouped per year and their average was calculated to obtain 70 Z_{it} values which were needed for succeeding calculation.

Southwest Monsoon Rainfall Anomaly Index. The spatial average for Z_i, the annual variation, at each station were calculated to derive a single index called the SWMRAI. For each year (t), SWMRAI is expressed as:

$$(2) \quad SWMRAI_t = \frac{1}{N}\sum_{i=1}^{N} Z_{it}$$

Where:
N = total number of stations in a particular year t
Z_{it} = standardized rainfall anomaly at year t

The data that were obtained from this step are 70 values – one SWMRAI value per year.

Standard deviation of SWMRAI. The standard deviation *s* of SWMRAI was also calculated to identify a threshold for determining the years with normal, above normal, and below-normal rainfall. The formula for standard deviation that was used is:

$$(3) \quad s = \sqrt{\frac{\sum_{i=1}^{n}(x_i - \bar{x_i})^2}{n-1}}$$

Where:
n = total number of stations
x_i = SWMRAI of each year
$\bar{x_i}$ = mean of x_i

The positive and negative *s* values were used as the upper and lower bounds. A year where the SWMRAI exceeds the positive *s* value means that the SWM rainfall at that year has above-normal rainfall and vice versa.

Standard deviation of annual rainfall data. The standard deviation of the total collected rainfall of year *t* in station *i* was calculated. A time-series graph of the SWM accumulated rainfall, taken as an average across all stations, was produced. Error bars were added to indicate the positive and negative standard deviation of annual rainfall data.

Safety Procedure. Protective measures were done to prevent the risk of file corruption as well as to ensure security. A copy of the files was downloaded directly from the email that PAGASA sent before any calculation was done and was stored in a virus-free flash drive. A copy of the original files was also uploaded to a Google drive folder, where files of calculated data were also stored.

Results and Discussion. - The average annual accumulated rainfall of all stations during the months of June to September, from the year 1949 to 2018 showed an inter-annual variability (see Figure 1). In the 70-year time series, a minimal increasing trend for the annual accumulated rainfall can be observed from its linear trend slope of +1.8047. The spatial variability which has a slope of -0.1065, however, indicates a decreasing trend. This implies that the degree to which rainfall amounts vary across time is decreasing. Great spatial variability can be observed in the years 1951, 1958, 1968, 1972, 1990, 2012, and 2018. It is also worth noting that the deviation between stations tends to be lower in years with lower accumulated rainfall. According to several studies [18,19], the observed interannual variability of rainfall is highly correlated to the effects of the El Niño Southern Oscillation. The shifting phenomenon of other monsoons in Southeast Asia also has an impact on rainfall variability [20]. Furthermore, The results for spatial variability are supported by the study of Cruz et al. [5] which also reported a decline in the linear trend of the spatial variability of total SWM rainfall from the year 1960 to 2010.

It can also be seen from Figure 1 that in 1972, the annual accumulated rainfall was significantly higher. This increase can be attributed to prolonged flood conditions due to the occurrences of tropical cyclones, further aggravated by the intensification of the SWM. The events that were primarily responsible for these conditions are Super Typhoon Rita and Typhoon Susan, which altered the monsoon winds over the Philippines. They were then succeeded by Typhoons Edeng, Gloring, Isang, and Huaning only weeks after. It is interesting to note that the 1972 great flood over Luzon occurred during an El Niño episode [21]. Villafuerte et al. [22] confirmed that with the development of El Niño in the north-central Philippines, wetter conditions during the months of July to September are expected.

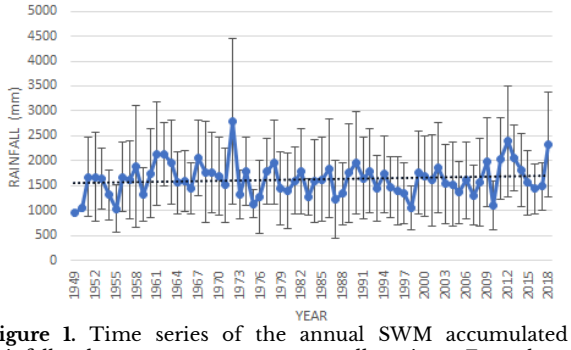

Figure 1. Time series of the annual SWM accumulated rainfall, taken as an average across all stations. Error bars indicate the standard deviation of station values. Dashed line indicates the linear trend.

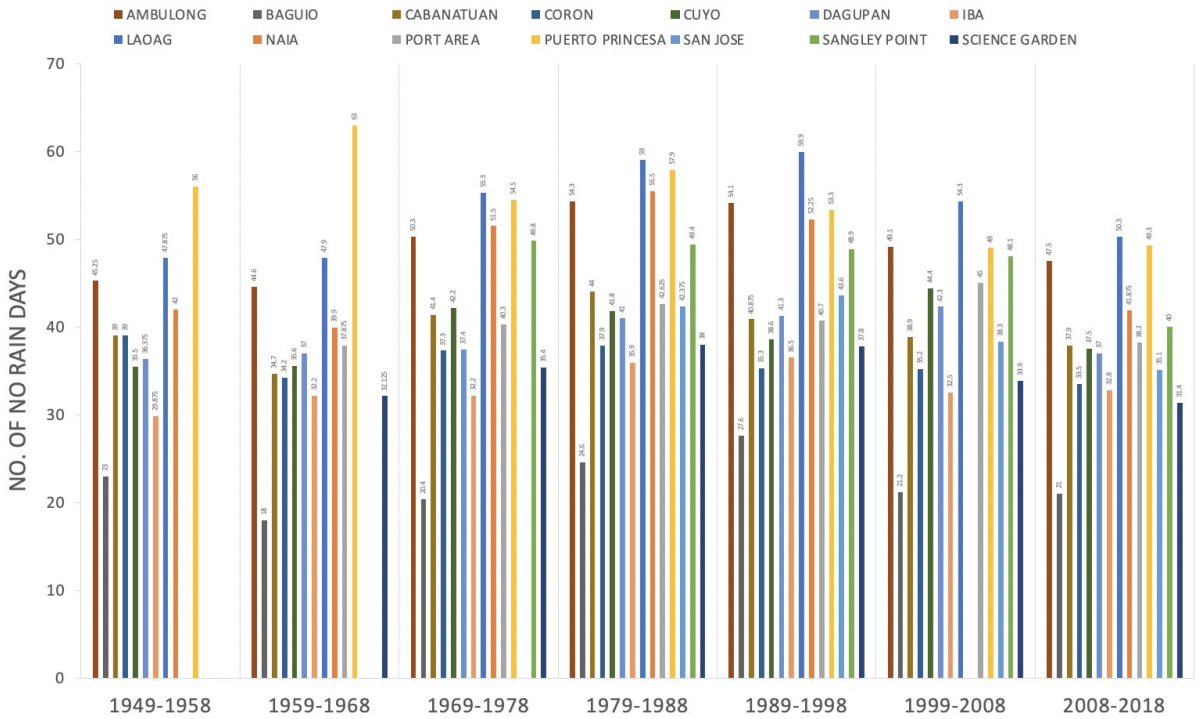

Figure 2. Decadal frequencies of no-rain days for the months of June to September from 1949 to 2018 for each station.

As seen in Figure 2, there is a decline in the frequency of no-rain days during SWM season for the past four decades (1979 to 2018), with the linear trend having a slope of -0.1177. The number of no-rain days has decreased from decades 1949–1958 and 1959–1968, increased from decades 1959–1968 to 1979–1988 and decreased from decades 1979–1988 to 2009–2018. It can be observed in the graph that in all stations, the years from 1979 to 1998 have the most number of no-rain days. Results also showed that the station in Iba received the most rain averaging 2887 mm per year, and the station in Puerto Princesa received the least rain averaging 708 mm per year for the past 70 years. Changes in the extremes are important to understand because of their climatic impact in terms of floods and droughts, which result in serious consequences especially on the agricultural and energy sectors [5].

Moreover, the decadal changes in the number of HPE days—those who are above the 85th, 95th, and 99th percentile (Figure 3)—are increasing as well. In other words, there is an overall increasing trend in the number of days belonging to the 85th, 95th, and 99th percentile rainfall throughout the decades. The slopes of their trends are +1.0586, +0.4740, and +0.1030, respectively. It can also be seen in the figures that all the trendlines have a positive slope, regardless of their percentile value. This indicates that rainfall has continually increased in terms of intensity within the 70-year period.

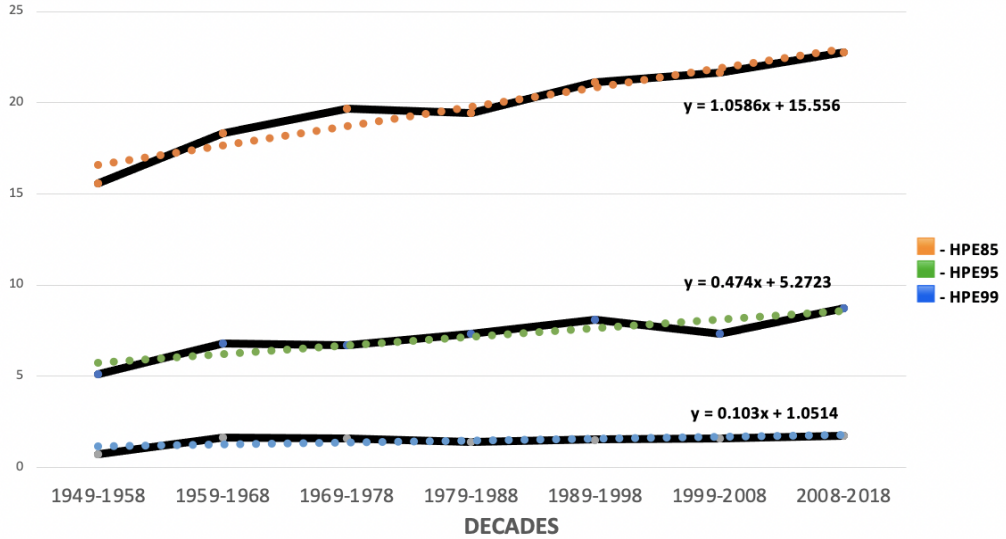

Figure 3. Overall trends of HPE85 (orange), HPE95 (green), and HPE99 (blue) days, defined as exceeding the 85th, 95th, and 99th percentile from 1949 to 2018, for the months of June to September for each station.

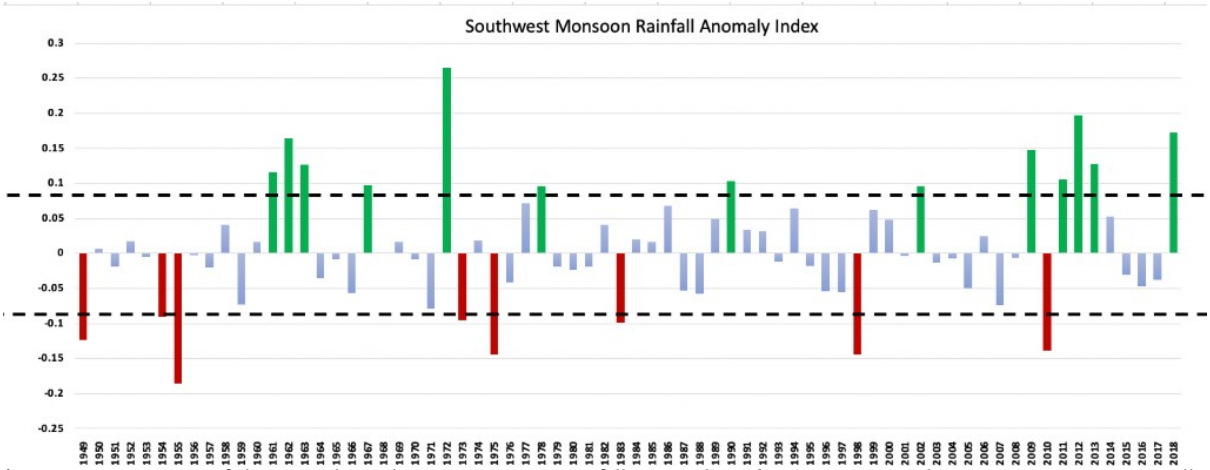

Figure 4. Time-series of the annual Southwest Monsoon Rainfall Anomaly Index (SWMRAI), taken as an average across all stations. The standard deviation of these indices (dashed line) sets the thresholds for normal rainfall. Years are classified as follows: above-normal (green), normal (blue), and below-normal (red).

Unlike the no-rain days graph, no station has consistently experienced the greatest or least HPE days. According to Cruz et al. [5], the 95th percentile of daily rainfall from the baseline climate is already considered as heavy rainfall. A negative trend in the 85th, 95th, and 99th percentiles of HPE days can be observed in their study, which is in contrast with our findings. However, this may be due to the difference in the number of stations and years analyzed. The study of Cruz et al. [5] utilized data from only 9 stations over a 50-year period, whereas this paper utilized data from 14 stations in a 70-year span.

As shown in Figure 4, the years with above-normal rainfall are 1961, 1962, 1963, 1967, 1978, 1990, 2002, 2009, 2011, 2012, 2013, and 2018, while the years with below-normal rainfall are 1949, 1954, 1955, 1973, 1975, 1983, 1998, 2010. The rest of the years are categorized under normal rainfall.

The standard deviation of SWMRAI, ±0.08460741, was used as the threshold in determining the years with above-normal and below-normal SWM rainfall. Within the 70-year period of study, 49 years were normal, 13 years were above-normal, and 8 years were below-normal. In the study of Cruz et al. [5], the majority of the years from 1961 to 2010 also fell in the normal rainfall category. Data from PAGASA was used in determining El Niño and La Niña years. Two (2) out of twelve (12) years when the Type 1 climate areas of the Philippines received above-normal rainfall, were La Niña years (1962, 1972). It is worth noting that one El Niño year (2002) belonged to the same category. One (1) out of eight (8) occurrences of below-normal rainfall were El Niño years (1983). Moreover, all except one below-normal rainfall years are La Niña years (1949, 1954, 1955, 1973, 1975, 1998, 2010). These findings show that El Niño years are not necessarily associated with below-normal rainfall, and the same idea can be applied to La Niña years as well.

Limitations. Not all stations had available rainfall data from 1949–2018 since they were constructed at different years, and some had to stop operations due to maintenance problems. This resulted in missing data in some years.

Conclusion. - During the Southwest monsoon season, there is an overall increase in the amount of rainfall and a decrease in drier days in Type 1 climate areas of the Philippines as compared to the past years. The frequency of no rain days has decreased, the trend lines observed in the frequency of high precipitation days at the 85th, 95th and 99th percentile are increasing, and the average accumulated Southwest monsoon rainfall has increased as well. The extremes in the number of no-rain days are the years from 1979 to 1998, and there are no extreme years for the number of HPE days in all three percentiles. This shows that during this period, a lot of days had zero precipitation, and for the years during this period that had above-normal rainfall, it can be inferred that precipitation was heavy during the rainy days. For the SWMRAI, 1955 is the year with the lowest recorded below-normal rainfall, while 1972 is the highest recorded above-normal rainfall value. The decrease in the frequency of no-rain days, and the increasing trend lines observed in the frequency of high precipitation days at the 85th, 95th, and 99th percentile, as well as the average accumulated Southwest monsoon rainfall shows that there is an overall increase in the amount of rainfall in the northwest portion of the Philippines during this season. It was found that whether a year falls in the below-normal, normal, or above-normal rainfall categorization is not dependent on its classification as an El Niño or La Niña event. In summary, based on the results of the data analysis, it can be concluded that there is a possibility of increased rainfall and shorter dry periods during the SWM season in future years. If the rainfall trend continues to increase in the future, heavy rainfall-related risks such as flooding and landslide occurrence are likely to escalate.

Recommendations. - Other factors such as passages of landfalling and non-landfalling tropical cyclones, wind, urbanization, and heat flux were not included in this study. An in-depth analysis on the correlation between other factors could provide better predictions for SWM rainfall. Lastly, it is recommended that sectors that are highly vulnerable to heavy rainfall, such as the agricultural sector, to regularly monitor the trend and prepare a risk management plan and risk reduction plan to help

them mitigate the negative effects of SWM in the future, since it is expected that rainfall will be heavier than previous years.

Acknowledgment. - The researchers would like to extend their gratitude to PAGASA for their punctuality in providing the rainfall data used in the study.

References

[1] Ohba M, Sugimoto S. 2019. Differences in climate change impacts between weather patterns: possible effects on spatial heterogeneous changes in future extreme rainfall. Clim Dyn. 52 (7–8). doi: 10.1007/s00382-018-4374.

[2] Olaguera LMP, Caballar ME, De Mata JC, Dagami LAT, Matsumoto J, Kubota H. 2021. Synoptic conditions and potential causes of the extreme heavy rainfall event of January 2009 over Mindanao Island, Philippines. Nat Hazards. https://doi.org/10.1007/s11069-021-04934-z.

[3] Boquet Y. 2017. A tropical archipelago. The Philippine archipelago. 37–59. doi:10.1007/978-3-319-51926-5_3.

[4] Cayanan EO, Chen TC, Argete JC, Yen MC, Nilo PD. 2011. The effect of tropical cyclones on Southwest Monsoon rainfall in the Philippines. J. Meteor. Soc. Japan. 89(A): 123–139. doi: 10.2151/jmsj.2011-A08.

[5] Cruz FT, Narisma GT, Villafuerte MQ, Cheng Chua KU, Olaguera LM. 2013. A Climatological Analysis of the Southwest Monsoon Rainfall in the Philippines. Atmos Res. 122. doi: 10.1016/j.atmosres.20 12.06.01

[6] Bagtasa, G. 2017. Contribution of Tropical Cyclones to Rainfall in the Philippines. J. Clim. 30 (10): 3621-3633. https://doi.org/10.1175/JCLI-D-16-0150.1

[7] Crost B, Duquennois C, Felter JH, Reese DI. 2018. Climate change, agricultural production and civil conflict: evidence from the Philippines. J Environ Econ Manag. 88 (2018): 379-395. https://doi.org/10.1016/j.jeem.2018.01.005.

[8] International Rice Research Institute. 2013. Rice Almanac 4th Edition. Retrieved 2021 Aug 10. Available from https://www.irri.org/resources/publications/books/rice-alamanac-4th-edition.

[9] Olesen JE, Trnka M, Kersebaum KC, Skjelvag AO, Seguine B, Peltonen-Sainiof P, Rossig F, Kozyrah J, Micale F. 2011. Impacts and adaptation of European crop production systems to climate change. Eu J Agron. 34(2):96–112. https://doi.org/10.1016/j.eja.2010.11.003.

[10] Cinco TA, de Guzman RG, Ortiz AM, Delfino RJ, Lasco R, Hilario F, Juanillo E, Barba R, Ares E. 2016. Observed Trends and Impacts of Tropical Cyclones in the Philippines. Int J Climatol. 36(14). doi: 10.1002/joc.46.

[11] Basconcillo JA. 2019. Gender and climate change adaptation: a case study of flood-prone rice-farming villages in Bulacan, Philippines. In: Paris TR, Rola-Rubzen MF, editors. Gender dimension of climate change research in agriculture: case studies in Southeast Asia. Philippines: SEARCA; Netherlands: CCAFS.

[12] Chan JCL. 2000. Tropical Cyclone Activity over the Western North Pacific Associated with El Nino and La Nina Events. J. Clim. 13(16). doi: 10.1175/1520-0442(2000)013<2960:TCAOTW>2.0.CO.

[13] Chen TC, Wang SY, Huang WR, Yen MC. 2004. Variation of the East Asian Summer Monsoon Rainfall. J. Clim. 17 (4). doi: 10.1175/1520-0442(2004)017<0744:VOTEAS>2.0.CO

[14] Zhang Y, Li J, Xue J, Zheng F, Wu R, Ha KJ, Feng J. 2019. The Relative Roles of the South China Sea Summer Monsoon and ENSO in the Indian Ocean Dipole Development. Clim Dyn. 53 (11). doi: 10.1007/s00382-019-04953.

[15] Racoma BAB, David CPC, Crisologo IA, Bagtasa G. 2016. The change in rainfall from tropical cyclones due to orographic effect of the Sierra Madre Mountain Range in Luzon, Philippines. Philipp J Sci. 145(4): 313–326.

[16] Bagtasa G. 2020. 118-year climate and extreme weather events of Metropolitan Manila in the Philippines. Int J Climatol. 40, no. 2(2020): 1228–1240.

[17] Wilks D. 1995. Statistical methods in atmospheric sciences. An introduction. Academic Press, San Diego, 467 pp.

[18] Feng J, Wang L, Chen W. 2014. How does the East Asian summer monsoon behave in the decaying phase of El Niño during different PDO phases? J Climate. 27(7): 2682–2698.

[19] Villafuerte M, Matsumoto J. 2015. Significant influences of global mean temperature and ENSO on extreme rainfall in Southeast Asia. J Climate. 28(5): 1905–1919.

[20] Loo Y, Billa L, Singh A. 2015. Effect of climate change on seasonal monsoon in Asia and its impact on the variability of monsoon rainfall in Southeast Asia. Geosci. Front. 6 (6): 817-823. https://doi.org/10.1016/j.gsf.2014.02.0.

[21] Hilario F, De Guzman R, Ortega D, Hayman P, Alexander B. 2009. El niño southern oscillation in the Philippines: impacts, forecasts, and risk management. Philipp J Dev. 66: 36(1).

[22] Villafuerte II, Marcelino Q, Matsumoto J, Akasaka I, Takahashi HG, Kubota H, Cinco TA. 2014. Long-term trends and variability of rainfall extremes in the Philippines. Atmos Res. 137(2014): 1–1.

Publiscience Vol. 4 Issue 1

Microplastics in farmed oysters (*Crassostrea iredalei*) from Capiz, Philippines

ARABELLA SHAYNE S. BRAÑA, MARIAMA LOIS P. CELESTIAL, RYNE JETHRO M. MOLINA, and CATHERINE JOY A. MEDIODIA

Philippine Science High School Western Visayas Campus - Department of Science and Technology (DOST-PSHSWVC), Brgy. Bito-on, Jaro, Iloilo City 5000, Philippines

Article Info

Submitted: May 02, 2021
Approved: Jul 24, 2021
Published: Aug 30, 2021

Keywords:
microplastic
oyster
Crassostrea iredalei
FTIR
KOH digestion

Abstract

Microplastics (plastic particles <5 mm in size) have been increasingly abundant, especially in filter-feeders. Oysters are commercially farmed and highly consumed in the Philippines. This study determined the presence of microplastics in commercial oysters (*Crassostrea iredalei*) sold in public markets from Cagay, Culajao, and Ivisan, Capiz. Thirty oysters yielded 47.6 g of meat, which were homogenized, divided into nine portions for KOH digestion, and incubated at 40 °C for 48 h. The digestates were passed through 25 µm Whatman filter paper. The retained particles were viewed under a microscope, identified by GESAMP descriptors, photographed, counted, and measured. Three residues were analyzed by FTIR spectroscopy to identify the chemical origin of the microplastics. The study confirmed the presence of microplastics in the oysters. The 38 microplastic particles were mostly fibers with some sheets. Their sizes ranged from 109 µm to 3.3 mm, and did not significantly differ among the three source locations. Only the sheet particle had a 49% match with cellophane.

Introduction. - Microplastics are plastic particles with sizes less than 5 mm that have become the most abundant pollutant in the aquatic environment [1,2]. Two types of microplastics exist: primary and secondary. Primary microplastics are those manufactured to size and secondary microplastics are tiny fragments from degraded larger plastics. Microplastics enter the seas directly as marine litter from shipping and fishing, or indirectly as solid wastes from land through rivers and estuaries [3, 4]. Encounters and interactions between microplastics and marine organisms are inevitable and problematic and such interactions will continue to increase as microplastics continue to accumulate over time [1].

Microplastics are imminent threats to marine biota because they are ingested and as a result, they have been found in the bodies of various marine animals including fishes [5,6] and bivalves [7,8], consequently causing digestive blockage, organ damage, low birth and growth rates, and reproductive failure [9,10]. Over time microplastics extend their effects to humans through the consumption of seafood [11] as a result of bioaccumulation]. The effects of microplastics on human health are unclear but the severity of adverse effects can depend on the toxicity of the chemicals used to produce the plastic [12].

There is huge potential for microplastics to adversely impact populations of marine animals and the Filipinos who consume them. Fish and other seafood account for 15.5% of the total protein intake in the Philippines [13] and the per capita consumption of crustaceans and mollusks is about 3 kg/year [14]. In 2019, Capiz is the top producer of fish and marine products in Western Visayas, including 31% of the aquaculture products from the region [15]. In Roxas City alone, mariculture areas produce about 513 metric tons of grouper, oysters, and mussels annually [16]. Thus, due to the considerable role of Capiz in producing commercial seafood, it is important to obtain data on microplastics found in farmed and marketed oysters (*Crassostrea iredalei*) from the aforementioned locale.

In summary, this study aims to identify and assess microplastics in commercial oysters (*C. iredalei*) from selected areas in Capiz. Specifically, it aims to:

(i) extract microplastics from oysters from three locations in Capiz;

(ii) describe, photograph, count, and measure the extracted microplastics;

(iii) identify the chemical origin of the microplastic particles; and

(iv) compare the microplastics found in oysters from the three locations.

The results of this study will benefit future studies that aim to further investigate and assess the

How to cite this article:
CSE: Braña AS, Celestial ML, Molina RJ. 2021. Microplastics in farmed oysters (*Crassostrea iredalei*) from Capiz, Philippines. Publiscience. 4(1): 8–13.
APA: Braña A.S., Celestial M.L., & Molina R.J.. (2021). Microplastics in farmed oysters (*Crassostrea iredalei*) from Capiz, Philippines. *Publiscience, 4*(1), 8–13.

For supplementary data, contact: publiscience@wvc.pshs.edu.ph.

presence of microplastics in marine environments and organisms. Furthermore, this study may also be a baseline for future studies concerning the occurrence of microplastics in the food chain. The use of KOH digestion adapted from Thiele et. al. [7] can be used as a reference for future bivalve tissue digestion for microplastic extraction.

Methods. - This study aims to identify and assess the presence of microplastics in *C. iredalei* through visual inspection, FTIR analysis, and statistical analysis.

Site Selection. Site selection was done through purposive sampling. Various seafood restaurants in Iloilo were contacted and inquired about their oyster supply, and most referred to Capiz as the source. Study sites were selected based on (1) the presence of oyster collectors or oyster farms; (2) availability and abundance of marketable oysters; (3) the oyster species was *C. iredalei*; and (4) presence of local sources of pollution. Three locations were then chosen- Cagay, Culajao, and Ivisan, Capiz (Figure 1) with the following latitude longitude coordinates: 11°35'47.8"N 122°46'39.2"E, 11°34'49.9"N 122°45'20.2"E, and 11°31'00.4"N 122°41'37.7"E respectively. All three locations had high levels of human populations, settlements, and commercial activities including fishing and fish farming.

Figure 1. Satellite image of the three sample locations taken using Google Maps.

Oyster Sampling. *C. iredalei* is easy to identify by its cup-shaped or slipper-shaped shell and the purple adductor muscle scar. The species identification was confirmed by the Southeast Asian Fisheries Development Center (SEAFDEC) in Tigbauan, Iloilo. Oyster samples were collected during the cool dry season (January, 2020) from a fish farm in Cagay and from the wet markets in Culajao and Ivisan, Capiz. A total of 15–20 oysters per site, all alive with shells shut tight. They were transported to PSHS-WVC and refrigerated at 3–6 °C for processing within 3 days. Ten live oysters of shell height 5–10 cm were chosen from each site sample for microplastic extraction. Oysters of this size were considered adults with well-developed digestive tracts, active feeding behavior, and high potential for ingestion of microplastics. The oysters were washed clean with tap water, blot-dried, then dissected in a laminar-flow cabinet to avoid contamination. To remove the oyster meat, the shell was opened by sliding a knife or scalpel between the valves and cutting the adductor muscle. The meat from 10 oysters from each site were pooled and weighed on an analytical balance. Oyster sizes (shell heights) did not differ significantly by location), but the larger oysters from Ivisan, Capiz yielded more meat.

Extraction of Microplastics. The pooled oyster meat from each source location was homogenized by combining the meat and divided into three equal weights in three beakers. The homogenates in nine beakers were chemically digested in a 10% w/v KOH solution at three times the meat volume [17]. The stock solution 10% KOH solution was prepared with 20 g KOH pellets dissolved in 200 ml distilled water. The homogenates were then incubated without agitation at 40°C for 48 h in an incubator (Biobase). Subsequently, the resulting digestates were poured on Whatman No. 4 qualitative filter paper with a pore size of 20–25 µm. The papers with residues were then placed in separate petri dishes, air-dried for 6 h and examined for microplastics. A blank sample, 10% KOH solution without oyster meat, was processed through all procedures to quantify possible microplastics contamination in the laboratory.

Visual Assessment by Microscopy. The residues were first subjected to visual assessment through microscopy at 40x magnification as the microplastic particles cannot be seen by the naked eye. The residues were viewed under a digital microscope connected to a laptop (Dell Inspiron 14 8th generation). Microplastics were identified and sorted by type according to the Joint Group of Experts on the Scientific Aspects of Marine Environmental Protection (GESAMP) [2] guidelines. The computer program Image Focus 4 was used to take images of the microplastics on filter papers. The microplastic particles were counted on 5x5 mm grids. The ImageJ and AmScope affiliate software were then used to measure the particle sizes.

FTIR Spectroscopy. Three of the extracted microplastics, named 'single fiber', 'fiber cluster', and 'sheet microplastic' were sent to the University of the Philippines Regional Research Center (UP-RRC) for Fourier Transform Infrared spectroscopy with a Thermo Scientific Nicolet iS5). This is in order to identify what type of plastic the microplastics originated from. The resulting FTIR spectra were compared or matched with the polymer database in the FTIR spectra library of UP-RRC. The analysis of the spectra was verified by a PSHS-WVC chemistry teacher.

Data Analysis. Data on oyster sizes and microplastic particle sizes were tabulated by source location and the means ± standard deviation were computed. The data were tested for normality via Shapiro-Wilk test. Furthermore, the means were compared by source location (one-way ANOVA at a 95% significance level). When the data were not normally distributed, the non-parametric Kruskal-Wallis test was used. All computations were done using the IBM® SPSS® Statistics v27 and RStudio© v3.6.1 software. The results were verified by a Statistics teacher from PSHS-WVC.

Safety Procedure. Use of personal protective equipment was observed during all laboratory work. Practice trials were conducted of all procedures from dissection of the oysters to extraction of microplastics

to microscopy. Furthermore, the empty oyster shells were bagged for disposal by the PSHS-WVC COOP personnel. Then, the used KOH solution was stored in plastic bottles and turned over to the Science Research Assistant at PSHS-WVC for proper disposal. Lastly, the researchers cleaned the work areas and organized the glassware after every use.

Results and Discussion. - This study aims to identify and assess microplastics in commercial oysters from selected areas in Capiz. Specifically, it aims to: (1) extract microplastics from oysters by means of KOH digestion and filtration; (2) describe, photograph, count, and measure the extracted microplastics under a digital microscope; (3) identify the chemical origin of the microplastic particles by spectroscopy; and (4) compare the microplastics found in oysters from three locations in Capiz.

Occurrence of Microplastics. A total of 38 microplastic particles were extracted from 47.6 g of meat from 30 oysters from the three sites in Capiz (Table 1). The data confirmed the occurrence of microplastics in farmed and marketed *C. iredalei* in Capiz — at least one microplastic particle per oyster regardless of source location. In other words, one microplastic particle was extracted for every 1.5 g of oyster meat.

Table 1. Counts and types of microplastic particles in oysters from three sites in Capiz, Philippines. (NO - Number of Oysters, TW - Total weight of oyster meat, TMPs - Total microplastics (NT + NS), NT - Number of threads, NS - Number of sheets)

Site	NO	TW (g)	TMPs (NT+NS)	NT	NS
Cagay	10	13.84	12	8	4
Culajao	10	15.48	15	13	2
Ivisan	10	18.28	11	10	1

This study confirmed the presence of microplastics in commercial oysters *C. iredalei* from raft farms and wet markets in Capiz, Philippines. Most particles were blue fibers, which are possibly remnants of fishing nets. Some were sheets that matched cellophane, a common packaging material. Cellophane is a polymeric cellulose film produced from processing cellulose from wood, cotton, hemp, or other sources. Some cellophane are coated with polyethylene or other polymers to make it heat sealable for automated wrapping machines. Though labeled as "biodegradable plastic," cellophane will break down completely only when being subjected to prolonged temperatures above 50 °C [10].

Particle Sizes of Microplastics. All the 38 (sum of all TMPs) extracted particles were <3.3 mm in their greatest dimension (Table 2) and thus were microplastic by definition. The smallest particle was 109 µm, which is much larger than the 20-25 µm pore size of the Whatman No. 4 filter paper that was used. The particle sizes apparently differed among locations, with mean sizes highest in Cagay and lowest in Ivisan (Table 2). However, the differences were not statistically significant (Kruskal-Wallis test, $p = 0.28$). Furthermore, a non-parametric test was used because the size data were not normally distributed (Shapiro-Wilk test, $p < 0.05$).

Table 2. Particle sizes (greatest dimension) of microplastics in oysters from three sites in Capiz. (NP - Number of Particles)

Sites	NP	Particle size (mm)			
		Min	Max	Mean	SD
Cagay	12	0.165	3.207	1.506	0.961
Culajao	15	0.123	2.928	1.266	0.967
Ivisan	11	0.109	3.260	0.951	0.975

The microplastics found in oysters in this study had particle sizes of 0.11–3.25 mm, larger than those (0.1–0.3 mm) found in green mussels in Bacoor Bay [18], but similar to those (0.56–4.58 mm) found in the waters of Pasig River [19]. Much smaller microplastics of sizes 2–6 µm adversely affected reproduction in the oysters studied by Sussarellu et. al. [20]. It remains to be determined whether smaller microplastics, and even the larger microplastics that were found, would also be harmful to *C. iredalei.*

Types and Composition. The microplastics left on the filter paper were mostly thin blue fibers but some were sheet-like and white or transparent. The 38 microplastic particles consisted of fibers (81.58%) with some sheets (18.42%) (Table 1). Digital images of the extracted microplastic particles are shown in Figure 1.

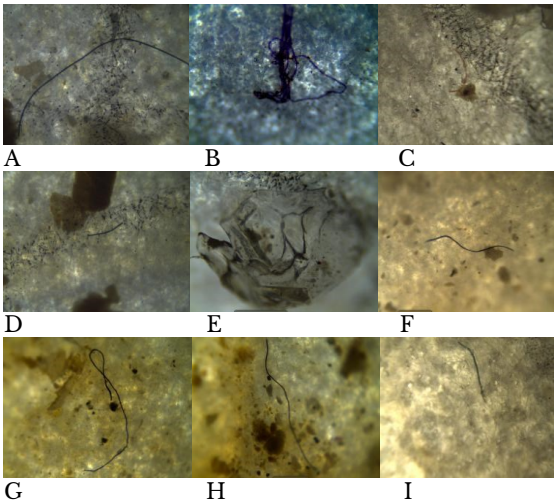

Figure 1. Microplastic particles extracted from farmed oysters from Capiz. Images taken by digital microscope of the residues on three filter papers per location. A-C Cagay; D-F Culajao; G-I Ivisan.

Indeed the study sites confirmed the extensive use of plastic nets, ropes, containers, and other gear in locations consume a variety of plastic products and packaging materials that were plainly visible as fishing and fish farming. Furthermore, it can be inferred that numerous households in the three

scattered litter: sachets of shampoo and coffee, single-use bags, wrappers, jars, etc. Markets and tourism and recreational activities were also sources of plastic pollution at the study sites.

Chemical Origin of Microplastics. The microplastics analyzed by FTIR spectroscopy are shown in Figure 5. 'Sheet microplastic' is image E. 'Single fiber' is image A and 'fiber cluster' is image G.

Figure 2 shows the FTIR spectrum of the 'sheet microplastic' together with the library matching, which yielded a 49% match with cellophane. A 49% match under normal conditions is not considered an ideal match rate, however, with the nature of these microplastic samples, it is deemed acceptable. The samples were dried insufficiently due to lack of supporting articles, and with this, saltwater residues and oxidized groups interfered in the results, thus producing a low match rate. In contrast, the FTIR spectra for 'single fiber' and 'fiber cluster' showed no match with any polymer in the database (Figures 3 and 4).

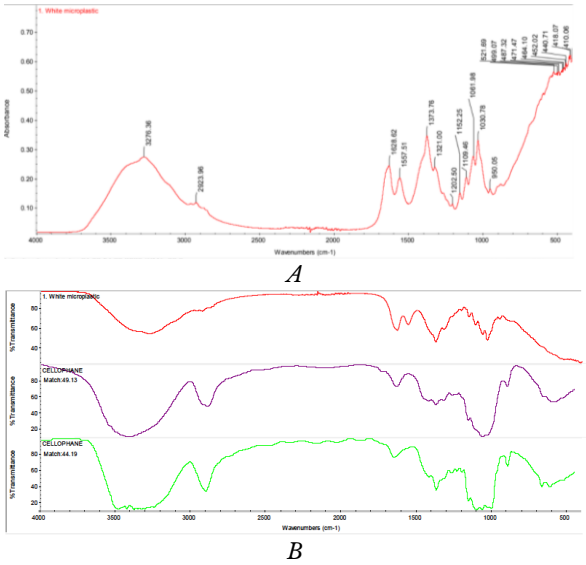

A

B

Figure 2. A The FTIR spectrum of sheet microplastic; B Library match with cellophane, 49%.

The fibers and sheets that were analyzed by FTIR spectroscopy could not be matched with any polymer in the UP-RRC spectra database. This result was probably due to insufficient drying of the fibers in the residue on the filter paper. Furthermore, the structural identity of the microplastic samples was also compromised given the changes in the chemical structures of the samples (e.g. bond breakage, etc.). Da Costa et al. [21] reported that the physical and chemical properties of a microplastic particle are affected by prolonged exposure to saltwater. The formation of oxidized groups from exposure to water results in noise when the spectroscopy test was conducted. While it is difficult to identify the primary causes of noise in spectroscopy, deficiencies in sample preparation/handling is considered a probable cause.

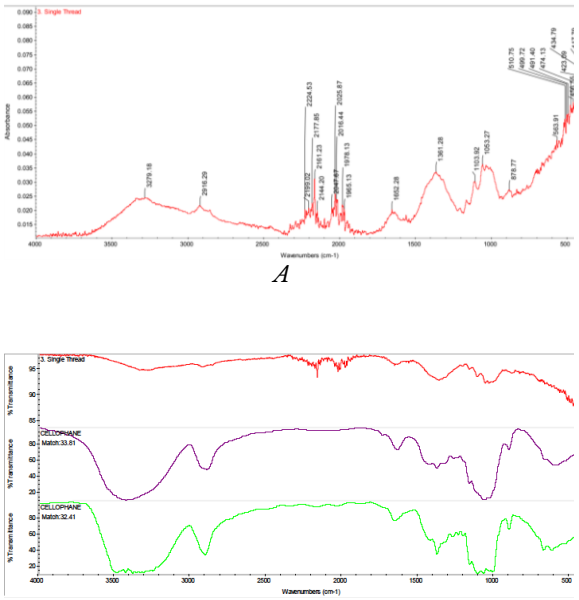

A

B

Figure 3. A The FTIR spectrum of 'single fiber' microplastic; B Library match not found.

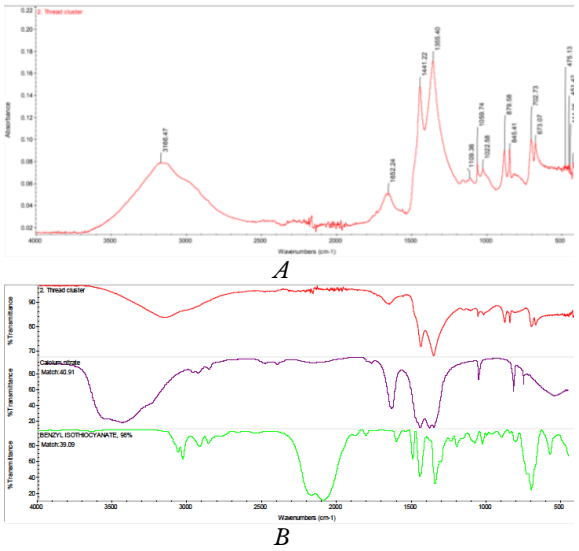

A

B

Figure 4. A The FTIR spectrum of 'fiber cluster' microplastic; B Library match not found.

Limitations. Cellulose filter paper was unavailable during the conduct of the laboratory procedures and Whatman® Grade 4 qualitative filter paper was used instead. Thus, particle retention was limited to 25 µm. Secondly, the Fourier Transform Infrared (FTIR) spectra were only compared to pre-identified polymer databases. Thus, other non-polymer spectra were not subjected for comparison.

Conclusion. - Microplastic presence was confirmed in commercial oysters *C. iredalei* collected from three various locations in Capiz with Culajao yielding the highest number of microplastics among the three locations. The abundance of microplastic fiber found and the identification of cellophane in 'white microplastic' suggest that the source of microplastics come from maritime activities such as fishing and improper disposal of household waste in the area. Statistical analysis concludes that the

location of the collection sites do not directly affect the microplastic size.

Recommendations. - To improve the study, it is recommended that cellulose filter paper with pore size lower than 25 µm should be used during filtration to enable the extraction of microplastics that have a diameter less than 25 µm. Additionally, air-drying the filter papers used during filtration at room temperature can be used as an alternative to oven-drying, which will greatly enhance the generated IR spectra as water will no longer be factored in the FTIR analysis. It is also recommended that a library match with a more extensive polymer library should be conducted to yield a more specific polymer type. Furthermore, the microplastics extracted may be weighed using more precise weighing scales to calculate microplastic abundance in milligrams microplastic/sample mass or for sediment studies, milligrams microplastic/kg^{-1} sediment. Finally, it is recommended that the results of this study are communicated to local government units to allow oyster farmers to reevaluate the conditions of their farm and create appropriate measures to reduce microplastic pollution such as imposing strict guidelines on proper waste disposal.

Acknowledgment. - We would like to extend our gratitude to Mrs. Junemie Ramos from SEAFDEC Iloilo for aiding us in the authentication of the oyster species. Likewise, we also extend our gratitude to Mr. Mark Rosales for responding to our queries and assisting us in our data presentation and analysis. Finally, we would also like to thank Mrs. Teodora Bagarinao for assisting us with our documents.

References

[1] Law KL, Thompson RC. 2014. Microplastics in the seas. Science. 345(6193): 144–145. doi:10.1126/science.1254065.

[2] GESAMP (Joint Group of Experts on the Scientific Aspects of Marine Environmental Protection). 2019. Guidelines for the Monitoring and Assessment of Plastic Litter in the Ocean. Nairobi, Kenya: United Nations Environment Programme (UNEP). p. 11–12.

[3] Eerkes-Medrano D, Thompson R, Aldridge D. 2015. Microplastics in freshwater systems: a review of the emerging threats, identification of knowledge gaps and prioritisation of research needs. 75: 63–82. https://doi.org/10.1016/j.watres.2015.02.012.

[4] Vermeiren, P, Munoz CC, Ikejima K. 2016. Sources and sinks of plastic debris in estuaries: A conceptual model integrating biological, physical and chemical distribution mechanisms. MarPollut Bull. 113: 7–16. https://doi.org/10.1016/j.marpolbul.2016.10.002.

[5] Bucol L, Romano E, Cabcaban S, Siplon LM, Madrid GC, Bucol A, Polidoro B. 2019. Microplastics in marine sediments and rabbitfish (Siganus fuscescens) from selected coastal areas of Negros Oriental, Philippines. Mar Pollut Bull. 148. https://doi.org/10.1016/j.marpolbul.2019.110685.

[6] Sarijan S, Azman S, Said MIM, Lee MH. 2019. Ingestion of microplastics by commercial fish in Skudai River, Malaysia. Environ Asia. 12(3): 75–84.http://dx.doi.org/10.14456/ea.2019.47.

[7] Li J, Yang D, Li L, Jabeen K, Shi H. 2015. Microplastics in commercial bivalves from China. Environ Pollut. 207: 190–195. https://doi.org/10.1016/j.envpol.2015.09.018.

[8] Ding J, Li JX, Sun CJ, He CF, Jiang FH, Gao FL, Zheng L. 2018. Separation and identification of microplastics in digestive systems of bivalves. Chinese J Anal Chem. 46(5): 690–697. https://doi.org/10.1016/S1872-2040(18)61086-2.

[9] Wright SL, Thompson RC, Galloway TS. 2013. The physical impacts of microplastics on marine organisms: a review. Environ. Pollut. 178: 483–492.https://doi.org/10.1016/j.envpol.2013.02.031.

[10] Cole M, Lindeque P, Fileman E, Halsband C, Galloway TS. 2015. The impact of polystyrene microplastics on feeding, function and fecundity in the marine copepod Calanus helgolandicus. Environ Sci Technol 49: 1130–1137. https://doi.org/10.1021/es504525u.

[11] Van Cauwenberghe L and Janssen CR. 2014. Microplastics in bivalves cultured for human consumption. Environ. Pollut. 193: 65–70. https://doi.org/10.1016/j.envpol.2014.06.010.

[12] Smith M, Love DC, Rochman CM, Neff RA. 2018. Microplastics in seafood and the implications for human health. Curr Environ Health Rep. 5(3): 375–386. doi: 10.1007/s40572-018-0206-z.

[13] Food and Agriculture Organization (FAO). 2020. Aquaculture growth potential in the Philippines. FAO. [accessed 2021 Mar 18]. Available from https://bit.ly/3g9lqbd.

[14] BFAR On-Line Information System. c 2018. Bureau of Fisheries and Aquatic Resources. [cited 2021 Mar 21]. Available from https://bit.ly/3pp55Db.

[15] Philippine Statistics Authority. c 2020. Capiz fishery production in 2019 [Internet]. [accessed 2021 Mar 18] https://bit.ly/3vXa94c.

[16] Baes MM. 2015. Economic analysis and adaptation measures of small-scale aquaculture in Roxas City, Capiz. University of the Philippines Visayas.

[17] Thiele CJ, Hudson MD, Russel AE. 2019. Evaluation of existing methods to extract microplastics from bivalve tissue: Adapted KOH digestion protocol improves filtration at single-digit pore size. Marine Pollution Bulletin. 142: 384–393.

https://doi.org/10.1016/j.marpolbul.2019.03.003.

[18] Argamino CR and Janairo JI. 2016. Qualitative assessment and management of microplastics in Asian green mussels (*Perna viridis*) cultured in Bacoor bay, Cavite, Philippines. Environment Asia. 9(2): 48–54. doaj.org/article:b0df33553e1b401492b3c50d526457ab.

[19] Deocaris CC, Allosada JO, Ardiente LT, Bitang LGG, Dulohan CL, Lapuz JKI, Padilla LM, Ramos VP, Padolina JBP. 2019. Occurrence of microplastic fragments in the Pasig River. H2Open Journal 2: 92–100. https://doi.org/10.2166/h2oj.2019.001.

[20] Sussarellu R, Suquet M, Thomas Y, Lambert C, Fabioux C, Pernet ME, Le Goïc N, Quillien V, Mingant C, Epelboin Y, et al. 2016. Oyster reproduction is affected by exposure to polystyrene microplastics. Proceedings of the National Academy of Sciences. 113: 2430–2435. https://doi.org/10.1073/pnas.1519019113.

[21] Da Costa J, Nunes A, Santos P, Girao A, Duarte A, Rocha Santos T. 2018. Degradation of polyethylene microplastics in seawater: insights into the environmental degradation of polymers. Journ of Environ Sci and Health. 53(9): 866–875. doi: 10.1080/10934529.2018.145.

Publiscience Vol. 4 Issue 1

Evaluation of the larvicidal efficacy of *Artocarpus heterophyllus* (jackfruit) rags and rind ethanolic crude extracts against third to early fourth instar *Aedes aegypti* larvae

BLESSY MARIE A. ALIBO, MYANNA SHAREE P. FUENTES, GYDEL FAITH A. ORBINA, and CATHERINE JOY A. MEDIODIA

Philippine Science High School Western Visayas Campus - Department of Science and Technology (DOST-PSHSWVC), Brgy. Bito-on, Jaro, Iloilo City 5000, Philippines Brgy. Bito-on, Jaro, Iloilo City 5000, Philippines

Article Info

Submitted: Apr 21, 2021
Approved: Jun 23, 2021
Published: Aug 30, 2021

Keywords:
Artocarpus heterophyllus
Aedes aegypti
biolarvicide
larvicidal bioassay
phytochemical analysis

Abstract

Artocarpus heterophyllus (jackfruit) is a shrub that has high phytochemical content in its different plant parts. However, 60% of its fruit remains underutilized. This study evaluated the larvicidal activity of the crude extracts of *A. heterophyllus* rags, rind, and combined rags and rind against third to early fourth instar *Aedes aegypti* larvae. Larvicidal bioassay was performed using concentrations ranging from 500–2500 ppm. Larval mortality data were recorded after 48 hours of exposure and were analyzed using Probit analysis. The *A. heterophyllus* rags and rind crude extracts showed high larval percent mortality rates of 70%-90%. The rind crude extract has the highest larvicidal efficacy since it has the lowest LC50 and LC90 values of 1136 ppm and 2500 ppm, respectively. The promising larvicidal activities shown by the treatments may be attributed to the abundance of triterpenes, saponins, tannins, and glycosides that was found using qualitative phytochemical analysis. Thus, the crude extracts of *A. heterophyllus* rags and rind may be used as alternatives to synthetic larvicides.

Introduction. - Dengue epidemics have increased for the past 20 years in both number and magnitude due to the rapid spread of the *Aedes aegypti* mosquito, the primary vector of dengue viruses, which thrives in highly urbanized areas [1]. The disease is one of the most significantly widespread mosquito-borne viral infections in humans [2]. Due to the lack of medical response against dengue viruses, effective vector control measures have become the sole weapon against dengue today [3]. The application of chemical insecticides to control the principal dengue vector, *Ae. aegypti*, is widespread. However, the development of resistance against these chemicals, the undesirable effects on non-target organisms, and the rise of environmental and health concerns led to the search for other alternative methods in controlling vector mosquitoes, such as the use of plants [4].

Plant-derived products have been used as insecticides in substitute for synthetic chemicals. They are less toxic, less prone to the development of resistance, and easily biodegradable [5]. The general classes of phytochemicals that they contain (sterols, triterpenes, flavonoids, alkaloids, saponins, glycosides, and tannins) are responsible for their insecticidal activity. These phytochemicals extend the postembryonic development of larvae and pupae and delay the formation of adult insects [6].

Artocarpus heterophyllus, also known as jackfruit, is a tree belonging to the mulberry family (Moraceae). It has naturalized in the tropics, particularly in Southeast Asia, and is considered an important crop in many countries such as the Philippines [7]. Only 15–20% of the ripe fruit is utilized as food [8], while 60% of the fruit which includes the rind, inner perdigones, and central core, are being thrown away as waste [9]. Thus, utilization of these parts must be done to convert these wastes into useful products [10].

Previous studies have focused on the pulp and seeds of the jackfruit and their phytochemical properties which reported that they have a high phytochemical content [11,12,13]. Moreover, the results of several studies have shown that high quantities of saponins, alkaloids, and flavonoids are present in jackfruits [11]. However, despite these pieces of information, none of the previous studies have isolated and examined the underutilized parts of jackfruit for their phytochemical content and larvicidal activity against dengue mosquito vectors,

How to cite this article:
CSE: Alibo BM, Fuentes MS, Orbina GF, Mediodia CJ. 2021. Evaluation of the larvicidal efficacy of *Artocarpus heterophyllus* (jackfruit) rags and rind ethanolic crude extracts against third to early fourth instar *Aedes aegypti* larvae. Publiscience. 4(1): 14–19.
APA: Alibo, B.M., Fuentes, M.S., Orbina, G.F., & Mediodia, C.J. (2021). Evaluation of the larvicidal efficacy of *Artocarpus heterophyllus* (jackfruit) rags and rind ethanolic crude extracts against third to early fourth instar *Aedes aegypti* larvae. *Publiscience*, *4*(1), 14–19.

For supplementary data, contact: publiscience@wvc.pshs.edu.ph.

specifically, the rags and rind of the fruit.

This study aimed to evaluate the larvicidal effect of *A. heterophyllus* crude extracts in terms of mortality rate against *Ae. aegypti* larvae. Specifically, the study aimed to:

(i) count the dead and moribund *Ae. aegypti* larvae after the treatment of *A. heterophyllus* rags, rind, and 50:50 combination crude extracts.

(ii) determine the lowest concentration of *A. heterophyllus* rags, rind, and 50:50 combination crude extracts that would yield 50% and 90% mortality rates in the larval population; and

(iii) assess and confirm the presence and abundance of phytochemicals in *A. heterophyllus* rags and rind using qualitative phytochemical analysis.

Methods. - The study conducted was experimental in nature. After the acquisition, *A. heterophyllus* rags, white or pale yellow fibrous strands surrounding the flesh, and rind, the green or yellow spiky outer skin of the fruit, were thoroughly rinsed before oven drying and powderization. The ground samples were macerated for 24 hours with constant agitation and filtered using vacuum filtration. Rotary evaporation was performed to obtain the crude extracts used in the succeeding processes. A qualitative phytochemical analysis was performed on both rags and rind samples to assess the active components. The larvicidal effect of each crude extract, against *Ae. aegypti* larvae were investigated using a larvicidal bioassay. Probit analysis was utilized to determine the LC50 and LC90 values of the crude extracts. The number of mosquito larval deaths in set-ups was recorded and counted manually after 24 hours and 48 hours of exposure.

Preparation of Samples. The samples were collected from a jackfruit vendor in Calle Real, Iloilo, and sent to the Department of Agriculture (DA) for verification. The rags and rind portion were separated, cut into smaller pieces, rinsed with distilled water, and oven-dried at 40 °C for 48 hours. The dried samples were ground into fine particles and weighed using a digital analytical balance.

Extraction. One hundred grams (100 g) of the ground samples were macerated in 1000 mL of 95% ethanol in amber glass bottles for 24 hours at room temperature. The solutions were mixed in batches using a magnetic stirrer and agitated at varying intervals. They were then filtered via vacuum filtration using Whatman Filter Paper no. 41. Subsequently, the samples were placed in a rotary evaporator at 40 °C until the ethanol completely evaporated. Lastly, the extracts were subjected to a flame test to verify the absence of ethanol in the samples.

Collection and Acclimatization of Test Organisms. Twenty (20) third to early fourth instar mosquito larvae were used for both the preliminary and final testing. The first and second instars of the larvae were not utilized as they are considered too fragile to handle.

The *Ae. aegypti* larvae used in the study were bred and cultured by the Department of Science and Technology-Industrial Technology Development Institute (DOST-ITDI) Entomology Section Insectary according to the standard procedures and general guidelines set by World Health Organization (WHO).

Preparation of Test Set-ups. Larval populations containing 20 organisms in each 100 mL glass beakers with 50 mL dechlorinated water were established. Relatively smaller and moribund larvae were replaced.

Preparation of Treatments. As specified in the Guidelines for Laboratory and Field Testing of Mosquito Larvicides of WHO, the quantity of the stock solution was obtained by diluting 1.5 grams of each of the *A. heterophyllus* extracts, namely: pure rags crude extract, pure rind crude extract, and the 50:50 combination, with 1.5 mL 95% ethanol and 13.5 mL water to achieve 100000 ppm or 10% w/v crude extract-ethanol solution [14]. The stock solutions were placed in 140 mL beakers. Shaking and stirring of the solutions were done to dissolve the extract with the solvent.

Abate® 1SG mosquito larvicide and 1% ethanol in dechlorinated water were used as positive and negative controls, respectively. These were then applied to the mosquito larvae set-ups.

Larvicidal Bioassay. The WHO standard protocol for testing the mortality of mosquito larvicides was followed. Two (2) preliminary experiments were conducted to establish the range of lethal concentrations that would be effective in killing 10% to 90% of the larval population. Each preliminary test contained five (5) test concentrations with three (3) replicates each. The final test concentrations were obtained on the second preliminary test, ranging from 500–2500 ppm. Six (6) replicates were carried out for each concentration. A water depth between 5–10 cm was maintained to prevent undue mortality when soaked in deeper levels [14,15]. Mortality data was recorded after 24 and 48 hours of exposure for each test set-up. The mortality rates were calculated using the formula below:

$$Mortality\ rate = \frac{Total\ number\ of\ dead\ larvae}{Initial\ number\ of\ larvae\ present} \times 100\%$$

Larvae that fail to display any immediate activity when probed or prompted were identified as dead or moribund [14].

Qualitative Phytochemical Analysis. Two hundred grams (200 g) of oven-dried *A. heterophyllus* rags and rind samples were sent to DOST-ITDI. The presence and abundance of the phytochemical components, specifically alkaloids, flavonoids, glycosides, saponins, sterols, tannins, and triterpenes were determined and assessed.

Data Analysis. Data from all replicates of each treatment were pooled for linear regression probit analysis using Microsoft® Excel® for Microsoft 365 MSO (16.0.13929.20360) 64-bit. The lethal concentrations to kill 50% and 90% of the larval

population, also known as LC50 and LC90 values, were determined by plotting the data points in a spreadsheet. The concentrations were then converted into logarithmic functions whereas the mean percentage of larval mortality adopted the corresponding probit values. A one-way Analysis of Variance (ANOVA) test was conducted at $\alpha = 0.05$ to statistically compare the treatments.

Waste Disposal. No chemical substances were disposed of down the drains. The containers with chemical wastes were placed in the chemical waste disposal box in the Biology Laboratory 2 of PSHS-WVC.

Stock solutions used in the larvicidal bioassay were disposed of in a separate container specifically for chemical waste while dead larvae were placed in biohazard containers. The standard procedures of the institution were followed. Beakers after testing were treated and sterilized with hot water.

Safety Procedure. The chemical and waste management were done according to the WHO Laboratory Safety Manual 4th Edition [16]. All laboratory chemicals and chemical wastes were treated with caution and exposure was minimized by observing laboratory safety measures such as wearing personal protective equipment (PPE) and conducting activities under the supervision of laboratory personnel. Chemical wastes were stored in properly-labeled closed containers. Extracts were properly stored in a 15 mL amber glass bottle.

Results and Discussion. - This study aimed to evaluate the larvicidal efficacy of the individual and combined crude extracts of *A. heterophyllus* rags and *A. heterophyllus* rind against third to early fourth instar *Ae. aegypti* larvae. This was done through a larvicidal bioassay. The data were collected after 48 hours for comparison and analysis.

Figure 1 shows the larvicidal activity of the three treatments against third to early fourth instar *Ae. aegypti* larvae by larvicidal bioassay. The three crude extracts showed significant toxicity based on the mean (%) mortality of the *Ae. aegypti* larvae. The mean (%) mortality of the three extracts increases as the concentration of treatments increases.

Two thousand five hundred (2500) ppm of *A. heterophyllus* rind extract has the highest mean (%) mortality. Five hundred (500) ppm of crude extracts of *A. heterophyllus* rags and of the combined *A. heterophyllus* rags and rind exhibited no larval death.

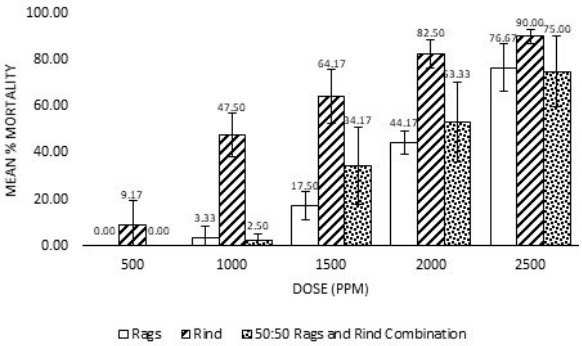

Figure 1. Larvicidal activity of the rind crude extract, rags crude extract, and 50:50 combination of rags and rind crude extract of *A. heterophyllus* against third and early fourth instar *Ae. aegypti* larvae after 48 hours.

Figure 2 shows the larvicidal activity of the positive control (Abate® 1SG larvicide) against third to early fourth instar *Ae. aegypti* larvae. The mortality of *Ae. aegypti* larvae was observed in all its concentrations with 0.3 ppm having the lowest mean (%) mortality at 10.00%, and 1.2 ppm having the highest at 96.67%. There was no larval mortality observed in the negative control treatment, 1% ethanol-dechlorinated water. The data show that all three crude extracts can be used as a larvicide. However, these are not as effective as the commercially available larvicide which is the positive control. Moreover, the results of the one-way ANOVA test showed that no significant difference exists between the groups determined by ($F(2,12) = 1.282$, $p = 0.3129$) at $\alpha = 0.05$. Thus, all extracts are equally effective.

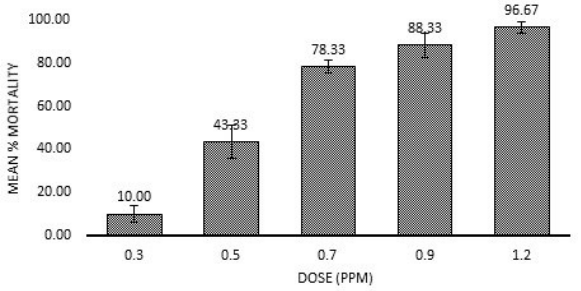

Figure 2. Larvicidal activity of the positive control, Abate® 1SG larvicide, against third to early fourth instar *Ae. aegypti* larvae after 48 hours.

Figure 3 shows the lethal concentrations of *A. heterophyllus* rags crude extract, *A. heterophyllu*s rind crude extract, and combined *A. heterophyllus* rags and rind crude extract against third to early fourth instar *Ae. aegypti* larvae after 48 hours of exposure.

The lowest LC50 and LC90 values were obtained from *A. heterophyllus* rind crude extract. The LC50 of *A. heterophyllus* rind crude extract was obtained at 1136 ppm while the LC90 was obtained at 2500 ppm. It was followed by combined *A. heterophyllus* rags and rind crude extract with LC50 and LC90 values of 1903 ppm and 3041 ppm, respectively. *A. heterophyllus* rags crude extract had its LC50 at 2012 ppm and LC90 at 3041 ppm.

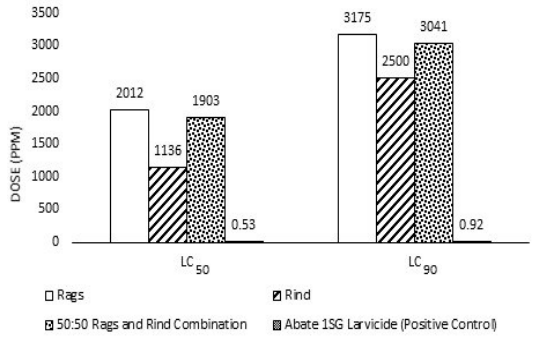

Figure 3. Lethal concentrations of different treatments against third to early fourth instar *Ae. aegypti* larvae after 48 hours of exposure period.

A. heterophyllus rind crude extract was the most effective larvicide among the three crude extracts for it has the lowest LC50 and LC90 values. The effectiveness of *A. heterophyllus* rind crude extract as a larvicide may be attributed to the abundance of known phytochemicals that are found in other plant-based larvicides in it.

A study conducted by Nair and Kavrekar [17] using the leaves of similar plant species was conducted and the results are more effective in terms of the LC50 and LC90. The LC50 and LC90 values of the treatment in the study are between 400 ppm and 600 ppm, and between 800 ppm and 900 ppm, respectively. The values mentioned are lower than the LC50 and LC90 values of the three treatments in this study [17]. Another study conducted by Pineda-Cortel et al. [18] made use of *Artocarpus blancoi* in different fractions and reported incomparable results with the result of the current study. Furthermore, the results of previous studies are more effective than the treatments used in this study.

The combination of crude extracts may exhibit synergistic or antagonistic effects. The combined extract used in this study, however, is only limited to one concentration which is 50:50. Other ratios were not studied in this study. Therefore, the best ratio to obtain a result that is more effective, in terms of the lethal concentration, than the individual extracts was not determined. The relationship of two crude extracts is synergistic when the quotient of the LC50 of the individual crude extract and of the combined plant crude extracts, also known as the synergistic factor, is greater than 1 [19]. The synergistic activity increases with the synergistic factor. In this study, the synergistic factor between the crude extracts of *A. heterophyllus* rags and the combined *A. heterophyllus* rags and rind crude extract is 1.057. On the other hand, the synergistic factor between the crude extracts of *A. heterophyllus* rind and the combined *A. heterophyllus* rags and rind is 0.597. This means that the crude extracts of *A. heterophyllus* rags and *A. heterophyllus* rind have an antagonistic relationship. This result is similar to the study of Grande et al. [20] where the combined extracts did not have an overall synergistic larvicidal effect against *Ae. aegypti* larvae. The LC50 and LC90 values of the combined extracts fell under the LC50 and LC90 values of the individual extracts. Based on the study, the failure of the combined extracts to have a synergistic effect on each other was due to the possible unforeseen chemical reactions between the phytochemicals that the individual extracts contain. However, this result differs in study of Yuan et al. [19] where the individual extracts exhibited a synergistic activity because the combined extracts were found to be a more effective larvicide than the individual extracts.

Table 1 shows the results of the qualitative phytochemical analysis of *A. heterophyllus* rags and rind. The results showed that *A. heterophyllus* rags crude extract does not contain sterols, flavonoids, and alkaloids. However, the rags extract has traces of saponins and glycosides, a moderate amount of tannins, and an abundance of triterpenes. The results also showed that *A. heterophyllus* rind crude extract does not contain sterols and alkaloids. Despite this, the rind extract contains traces of flavonoids and glycosides, and an abundance of triterpenes, saponins, and tannins.

Table 1. Qualitative phytochemical analysis of *A. heterophyllus* rags and *A. heterophyllus* rind samples.

Phytochemical	*A. heterophyllus* rind	*A. heterophyllus* rags
Sterols	(-)	(-)
Triterpenes	(+++)	(+++)
Flavonoids	(+)	(-)
Alkaloids	(-)	(-)
Saponins	(+++)	(+)
Glycosides	(+)	(+)
Tannins	(+++)	(++)

Traces (+), Moderate (++), Abundant (+++), Absent (-)

Saponins are known to decrease the digestive enzyme activity of mosquito larvae [21] and attack the cuticle membrane of the larvae [22]. Moreover, flavonoids attack the nerves and respiratory system of mosquito larvae [21]. Lastly, tannins form complexes with the digestive enzymes in the gut of insects which reduce the digestion efficiency and inhibit the growth of insects [22]. Previous studies have concluded that the abundance of saponins and tannins in plant extracts is responsible for the larvicidal activity of the plant extract [18,23,24].

In this study, the positive larvicidal activity exhibited by the three crude extracts was attributed to the presence of phytochemicals. Similar to previous studies, saponins, flavonoids, and tannins disrupted the normal body functions of larvae. The abundance of saponins and tannins in *A. heterophyllus* rind crude extract made it more effective than the other two crude extracts having a lesser amount of the mentioned phytochemicals present. Also, flavonoids are present in *A. heterophyllus* rind crude extract but not in *A. heterophyllus* rags crude extract. This is also a factor as to why *A. heterophyllus* rind crude extract is more effective as larvicide at a lower concentration than *A. heterophyllus* rags crude extract. Furthermore, the disruption of the normal body functions of the larvae decreased the health of the larvae and eventually caused the mortality of the larvae.

Limitations. The qualitative phytochemical test of DOST-ITDI only included a predetermined list of phytochemical components that were to be assessed in the plant samples. Thus, limiting the assessment to seven (7) components. The presence nor abundance

of other phytochemicals was not confirmed through the said test.

Conclusion. - The current study found *A. heterophyllus* rags, *A. heterophyllus* rind, and combinations of *A. heterophyllus* rags and rind crude extract as equally effective larvicides against third to early fourth instar *Ae. aegypti* larvae. The individual *A. heterophyllus* rind crude extract is the most efficient among the three treatments because it requires the least amount of concentrations to result in 50% and 90% mortality rates in the larval population. Phytochemicals were also found to be present in *A. heterophyllus* rags and rind, with the rind containing more phytochemicals. This is the reason why *A. heterophyllus* rind is more effective than *A. heterophyllus* rags. Therefore, the crude extracts of *A. heterophyllus* rags, *A. heterophyllus* rind, and a combination of *A. heterophyllus* rags and rind can be used as an alternative to synthetic larvicides.

Recommendations. - The researchers recommend that more replicates of each concentration for each treatment are to be used so as to eliminate outliers in the results. Other vector species may also be utilized as test organisms and various parts of the plant such as the leaves, bark, and seeds may be maximized for future studies involving a similar research design. The incorporation of essential oils in the treatments may also be considered. Furthermore, this study serves as a basis for future analyses on the active compounds present in *A. heterophyllus* rind and rags. Thus, it is recommended that an in-depth approach be conducted to further explore and identify the phytochemical components present in *A. heterophyllus*.

Acknowledgment - The researchers would like to extend their utmost gratitude to Mrs. Alicia Garbo and the personnel of the DOST-ITDI Standards and Testing Division for their close supervision. The knowledge imparted to and time allotted for the researchers are very much appreciated. They would also like to thank the vendors in Calle Real, Iloilo for entertaining and providing the needs of the researchers.

References

[1] Brown JE, Evans BR, Zheng W, Obas V, Barrera-Martinez L, Egizi A, Zhao H, Caccone A, Powell JR. 2014. Human impacts have shaped historical and recent evolution in *Aedes aegypti*, the dengue and yellow fever mosquito. Evolution. 68(2): 514–525. doi: 10.1111/evo.12281.

[2] Bhatt S, Gething PW, Brady OJ, Messina JP, Farlow AW, Moyes CL, et al. 2013. The global distribution and burden of dengue. Nature. 496(7446): 504–507. doi: 10.1038/nature12060.

[3] Bäck AT, Lundkvist A. 2013. Dengue viruses - an overview. Infection Ecology & Epidemiology 3:1, 19839. doi: 10.3402/iee.v3i0.19839.

[4] Hayes JB, Laws ER. 1991. Handbook of pesticide toxicology. San Diego: Academic Press.

[5] Prahbu K, Murugan K, Nareshkumar A, Ramasubramanian N, Bragadeeswaran S. 2011. Larvicidal and repellent potential of *Moringa oleifera* against malarial vector, *Anopheles stephensi* Liston (Insecta: Diptera: Culicidae). Asian Pac J Trop Biomed 1(2): 124–129. doi: 10.1016/S2221-1691(11)60009-9.

[6] Upadhyay RK. 2016. Botanicals; Its Safe Use in Pest Control and Environmental Management. Intern J Zool Invest. 2(1): 58–102.

[7] Elevitch CR, Manner HI. 2006. *Artocarpus heterophyllus* (jackfruit), verI.IV. In: Elevitch CR. (ed.). Species Profiles for Pacific Island Agroforestry. Permanent Agriculture Resources (PAR), Holualoa, Hawai'i. Available from: http://bit.ly/agroforestryorg.

[8] Silva JHV, Filho J, Ribeiro M, Silva EL. 2007. Effect of the addition of jackfruit (*Artocarpus heterophyllus* Lam.) seeds bran in dietary on the egg production, yolk pigmentation and dropping humidity in Japanese quais. Ciência Agrotécnica. 31: 523–530. doi: 10.1590/S1413-70542007000200037.

[9] Subburamu K, Singaravelu M, Nazar A, Irulappan I. 1992. A Study on the Utilization of Jackfruit Waste. Short Communication Bioresource Technology. 40: 85-86.

[10] Begum R, Aziz MG, Uddin MB, Yusof YA. 2014. Characterization of Jackfruit (*Artocarpus heterophyllus*) Waste Pectin as Influenced by Various Extraction Conditions. Agriculture and Agricultural Science Procedia. 2: 244–251. doi: 10.1016/j.aaspro.2014.11.035.

[11] Gupta D, Mann S, Sood A, Gupta RK. 2011. Phytochemical, nutritional and antioxidant activity evaluation of seeds of jackfruit (*Artocarpus heterophyllus*). International Journal of Pharma and Bio Sciences. 2(4): 333–343.

[12] Shanmugapriya K, Saravana S, Payal H, Mohamed P, Binnie W. 2011. Antioxidant activity, total phenolic and flavonoid contents of *Artocarpus heterophyllus* and *Manilkara zapota* seeds and its reduction potential. International Int J Pharm Pharm Sci. 3(5): 256–260.

[13] Abu Bakar MF, Abdul Karim F, Perisamy E. 2015. Comparison of phytochemicals and antioxidant properties of different fruit parts of selected Artocarpus species from Sabah, Malaysia. Sains Malaysiana. 44(3): 355–363. doi: 10.17576/jsm-2015-4403-06.

[14] [WHO] World Health Organization. 2005. Guidelines for laboratory and field testing of mosquito larvicides. Document WHO/CDS/CSR/LYO/2004.11. Geneva: World Health Organization.

[15] [WHO] World Health Organization. 2004. Laboratory safety manual. Document WHO/CDS/WHOPES/GCDPP/13. Geneva: World Health Organization.

[16] Pineda-Cortel MRB, Cabantog RJR, Caasi PM, Ching CAD, Perez JBS, Godisan PGM, Latorre CMG, Lucero DR, Salonga RB. 2019. Larvicidal and ovicidal activities of *Artocarpus blancoi* extracts against *Aedes aegypti*. Pharmaceutical Biology, *57*(1): 120–124. doi: 10.1080/13880209.2018.1561727.

[17] Nair S, Kavrekar V. 2017. In Vitro screening of larvicidal and insecticidal activity of methanolic extracts of Artocarpus heterophyllus, *Artocarpus altilis* and Piper betle. IJEAB. 2(1): 281–288. doi: 10.22161/ijeab/2.1.37.

[18] Pineda-Cortel MR, Cabantog RJ, Caasi P, Ching CA, Perez JB, Godisan PG, Latorre CM, Lucero D, Salonga R. 2019. Larvicidal and ovicidal activities of *Artocarpus blancoi* extracts against Aedes aegypti. *57*(1): 120–124. doi: 10.1080/13880209.2018.1561727.

[19] Yuan Y, Li L, Zhao J, Chen M. 2020. Effect of Tannic Acid on Nutrition and Activities of Detoxification Enzymes and Acetylcholinesterase of the Fall Webworm (Lepidoptera: Arctiidae). Journal of Insect Science. 20(1): 1–7. doi: 10.1093/jisesa/ieaa001.

[20] Grande RM, Balmaceda MD, Tanena MT, Mediodia H. 2019. Larvicidal activity of individual and combined ethanolic extracts of *Annona muricata* (Soursop) seed and Piper betle (Betel) leaf against *Aedes aegypti*. Publiscience 2(1): 73–76.

[21] Koneri R, Pantororing HH. 2016. Assay of Mahogani (*Swietenia macrophylla*) seed extract on Larvae of *Aedes aegypti* as Dengue Hemorrhagic fever vector. Jurnal MKMI. 12(4): 216–233.

[22] Jawale C. 2014. Larvicidal activity of some saponin containing plants against the dengue vector *Aedes aegypti*. DAMA International. 3(1): 1–11.

[23] Adewole A, Oderinde A, Bankole O, Farapusi F, Oyede RT. 2013. Larvicidal activities of three plant extracts of common wireweed *(Sida acuta*), Catnip (*Nepeta cataria*) and Neem (*Azadirachta indica*) against the larva of mosquito (*Anopheles gambiae*). Academia Journal of Medicinal Plants, 1(2): 37–40. doi: 10.15413/ajmp.2012.0106.

[24] Khanna VG, Kannabiran K. 2007. Larvicidal effect of *Hemidesmus indicus*, *Gymnema sylvestre*, and *Eclipta prostrata* against *Culex quinquefasciatus* mosquito larvae. Afr. J. Biotechnol. 6(3): 307–311. eISSN: 1684-5315.

[25] Carigaba MA, Leonida MA, Masculino CJ, Mediodia CJ, Garbo, AG. 2020. Larvicidal activity of *Citrofortunella microcarpa* (calamansi) peel essential oil against third and early fourth instar *Aedes aegypti*. Publiscience. 3(1): 37–41.

Publiscience Vol. 4 Issue 1

Reduction of acrolein concentrations in palm cooking oil emissions through the addition of *Muntingia calabura* (aratiles) leaf extract to inhibit lipid peroxidation

AMOS NATHAN B. TUANGCO[1], FRANCINE T. TARRAZONA[1], MARIA ZYKA J. YAMOG[1], ARIS C. LARRODER[1], and JADE G. PAHILA[2]

[1]*Philippine Science High School Western Visayas Campus - Department of Science and Technology (DOST-PSHSWVC), Brgy. Bito-on, Jaro, Iloilo City 5000, Philippines*
[2]*Food Science Laboratory, Regional Research Center, University of the Philippines Visayas, Miagao, Iloilo, Philippines*

Article Info

Submitted: Apr 19, 2021
Approved: Jun 24, 2021
Published: Aug 30, 2021

Keywords:
cooking oil fumes
acrolein
natural antioxidants
induction time
oxidative stability

Abstract

Inhaling acrolein, an aldehyde present in cooking oil fumes, is detrimental to human health. Fatty acids in oils can undergo the degradation process of oxidation, which produces acrolein and other volatile aldehydes. To prevent such degradation, plant-based antioxidants could be added to the oil. This study aimed to measure and compare acrolein concentrations in emissions of palm oil with varying concentrations (w/w) of *Muntingia calabura* ethanol leaf extract. Four set-ups were subjected to volatilization and dissolution through Rancimat analysis. Volatile oxidation products from the Rancimat were analyzed for acrolein through high-performance liquid chromatography. Results showed that acrolein concentrations decreased as the concentration of the leaf extract in the oil treatment increased. Thus, the addition of *M. calabura* leaf extract to palm oil has the potential of controlling oxidation during cooking by reducing acrolein emissions; safer kinds of cooking oil could be formulated with the preference of incorporating natural antioxidants.

Introduction. - Inhaled fumes from degrading cooking oil is a major matter of concern worldwide [1,2] due to their detrimental effects on the health of people staying indoors [2,3,4], particularly in the Philippines [5]. Mitigating the effects of indoor air pollution from oil-based cooking is important as people spend more than 90% of their time indoors [6,7,8], especially during the COVID-19 pandemic [9]. Meanwhile, among the air pollutants, aldehydes and polycyclic aromatic hydrocarbons are found to be the major products of oil degradation [3] and the most harmful [10,11,12].

As cooking oil is heated beyond its threshold smoke point, fatty acids present in oil oxidize rapidly to form aldehydes and free radicals [12]. However, the smoke point of the oil is not a reliable basis of aldehyde formation, as the formation of volatile organic compounds occurs before the temperature of the oil reaches the smoke point [13]. Oxidative stability is the better indicator of oil performance [13] since it is measured in terms of the time it takes for oils to start generating volatile secondary reaction products (induction time) before the temperature reaches the smoke point [14]. In addition, the rate of production of aldehydes is inversely related to the oxidative stability [12,15] of the cooking oil and directly related to cooking temperatures [3], fatty acid content [16], and atmospheric oxygen [17]. Hence, in this study, the relationship between oxidative stability and the amount of aldehydes emitted by the treated palm cooking oil samples was investigated.

Most of the studies conducted on cooking oil have focused on the improvement of its oxidative stability [15,18], but there has been none in reducing the harmful constituents found in cooking oil fumes. In relation to aldehyde formation, studies have postulated a possible association between the addition of natural antioxidants to cooking oil and the amount of aldehydes released by cooking oil when heated [12,18]. This is because the production of aldehydes can be inhibited through the use of antioxidants by bonding towards the singlet oxygen in the reaction intermediate as fatty acids degrade, as established by the same studies. The cooking oil emissions will be analyzed for acrolein, the simplest unsaturated aldehyde and the most abundantly produced by palm oil and soybean oil [12]. With this, it is necessary to examine the correlation between the addition of natural antioxidants and acrolein emissions.

Among various methods to inhibit oxidation, the use of antioxidants is most effective, convenient, and economical [19]. Between the natural and the synthetic antioxidants, the former are safer for

How to cite this article:
CSE: Tuangco ANB, Tarrazona FT, Yamog MZJ, Larroder AC, Pahila JG. 2021. Reduction of acrolein concentrations in palm cooking oil emissions through the addition of *Muntingia calabura* (aratiles) leaf extract to inhibit lipid peroxidation. Publiscience. 4(1): 20–25.
APA: Tuangco, A.N.B., Tarrazona, F.T., Yamog, M.Z.J., Larroder, A.C., & Pahila J.G. (2021). Reduction of acrolein concentrations in palm cooking oil emissions through the addition of *Muntingia calabura* (aratiles) leaf extract to inhibit lipid peroxidation. *Publiscience*, *4*(1), 20–25.

For supplementary data, contact: publiscience@wvc.pshs.edu.ph.

consumption due to toxicity problems associated with synthetic antioxidants [20]. Several studies investigated the effects of incorporating plant-based extracts, such as that from *Eucalyptus globulus* leaves, *Cinnamomum zeylanicum* bark, and *Sesamum indicum* coat, on the oxidative stability of cooking oil, resulting in longer induction times [15,18,20]. *Muntingia calabura* (aratiles) is one of the top five Philippine fruits to contain high antioxidant activity alongside *Diospyros blancoi* (velvet apple), *Tamarindus indica* (tamarind), *Sandoricum koetjape* (lolly fruit), and *Annona squamosa* (sugar apple) [22,23], making its extract a highly suitable additive, especially its leaves where the highest antioxidative activity can be found [24]. It is hypothesized that if *M. calabura* leaf extract is added to palm cooking oil (PCO), then its acrolein emissions will be reduced as an effect of the increase in its oxidative stability.

To address the issue of aldehyde emissions, this study aimed to measure and compare the acrolein concentrations in cooking oil fumes from palm oil with varying percent mass of *M. calabura* leaf extract. This study specifically aimed to:

(i) Determine the radical scavenging activity (RSA) and total phenolic content (TPC) of the *M. calabura* leaf extract through 2,2-diphenyl-1-picrylhydrazyl (DPPH) UV-visible radical scavenging assay;

(ii) Measure the induction time and antioxidative activity index (AAI) of the set-ups through Rancimat analysis;

(iii) Quantify the aldehyde concentrations derived from the fumes of the set-ups through high-performance liquid chromatography (HPLC);

(iv) Determine if there are significant differences among the induction times of the set-ups; and

(v) Determine if there are significant differences among the aldehyde concentrations from the fumes of the set-ups.

Methods. - The methods of this experimental study are composed of: (1) leaf harvesting and extraction, (2) DPPH assay, (3) treatment of oil samples, (4) Rancimat analysis, and (5) HPLC analysis. Four set-ups were prepared, with one set-up as the negative control and the other three as treatments.

Leaf Harvesting and Extraction. *M. calabura* leaves were washed and air-dried for one day, processed into smaller chunks, then transferred into a reagent bottle with 99% ethanol, following a 1:20 leaf to solvent ratio (w/v). The bottles were stored in a cool area for five days. Subsequently, the solution underwent vacuum filtration and rotary evaporation (60 °C heating bath temperature, 90 rpm, 5 hours). Lastly, the solution was reconstituted and air-dried in an exhaust for 3 days.

DPPH Assay. The RSA and TPC of the *M. calabura* leaf extracts were calculated through DPPH radical scavenging assay. Gallic acid was used as a standard to calculate the TPC. An extract-ethanol solution series (40, 80, 120, 160, 200 ppm) and a gallic acid solution (40 ppm) were prepared. Four milliliters (4 mL) of 0.1 mM DPPH-ethanol solution was added to 1 mL of each solution. All solutions were wrapped with aluminum foil and stored for 30 minutes in a cool dark area before the analysis. Absorbance values of the extracts and gallic acid were measured at a wavelength of 508.40 nm using a UV-vis spectrophotometer (Shimadzu UV-1800).

Treatment of Oil Samples. Four set-ups consisting of PCO samples with 0, 0.1%, 0.3%, and 0.5% mass of *M. calabura* leaf extract were prepared to achieve a total of 25 g. The maximum treatment concentration of 0.5% was based on the study of Mohamed et al. [25], which considered the limitations in the amount of additives safe for consumption. Oil samples were agitated for 5 minutes in an up-and-down motion before the analysis.

Rancimat Analysis. The Rancimat (Metrohm 892 Professional Rancimat) was set to a temperature of 150 °C and heated until it was stable to prevent temperature fluctuation. The gas flow of oxygen was set at the default setting of 20.0 L/hr while 60 mL of pure water (Merck, Elix Type II) was poured into each measuring vessel. The reaction vessels containing 3 g of the samples were heated in their respective heating blocks until the last sample had reached the stop criteria of 400 µS/cm conductivity. After 5 hours of heating, the resulting water samples were collected for further analysis of aldehydes. A total of 4 replicates were performed.

HPLC Analysis. Acrolein concentrations in the samples obtained from Rancimat analysis were determined through HPLC analysis (Shimadzu Prominence LC-20A UFLC Stack HPLC System), equipped with a UV-vis detector and a C8 150 x 4.6 mm 5µm column kept at 25 °C in the column oven. The analysis was carried out using an isocratic mode of elution using vacuum filtered distilled water as a mobile phase at a 2.0 mL/min flow rate. HPLC-grade acrolein (CPI International) standard solution (3, 6, 9, 12, and 15 ppm) was used to establish the calibration curve for quantification. The filtered (0.45 µm) samples were individually kept in a glass vial filled up to 2 mL volume, while 20 µL aliquots per sample were collected by the autosampler for analysis. A total of 4 replicates for each treatment were performed.

Computation of Parameters. The absorbance values obtained from the UV-vis spectrophotometer were used to calculate the RSA of the extract and gallic acid using Equation 1.

$$(1) \quad \%\ Inhibition = \frac{\lambda_{blank} - \lambda_{sample}}{\lambda_{blank}} \times 100\%$$

where λ_{blank} is the wavelength of the DPPH solution at maximum absorbance, and λ_{sample} is the wavelength of the DPPH-extract solution.

The TPC of the extract was calculated from the RSA of both gallic acid and the extract as shown in Equation 2.

$$(2) \quad TPC\ (\text{mg GAE/g}) = \frac{R_E \times 100}{R_G \times M_E}$$

where R_E is the RSA of the extract, R_G is the RSA of gallic acid, and M_E is the mass of extract used to calculate R_E.

Lastly, the AAI of the extract was calculated using Equation 3 [14].

$$(3)\quad AAI = \frac{I_{treatment}}{I_{control}}$$

where $I_{treatment}$ is the induction time of the treatment group and $I_{control}$ is the induction time of the control group.

Data Analysis. One-way analysis of variance (ANOVA) at α=0.05 was performed to determine if a significant difference exists between the percent mass extract in oil and the induction time among the four set-ups, as well as between the percent mass extract in oil and the acrolein concentration in its emissions. Pairwise comparisons using t-tests were then conducted to calculate the *p*-values between set-ups. All statistical analyses were performed using R software (RStudio®, v1.2.5033).

Safety Procedure. The samples and solutions were prepared under a fume hood. Personal protective equipment was worn at all times whenever handling reagents, samples, glassware, and equipment. Adherence to the respective safety data sheet of the chemicals was also observed. The use of equipment was done with proper protocol and training. Chemical and biological waste were placed in their respective waste containers to prevent further chemical reactions.

Results and Discussion. - After the DPPH assay was performed, the RSA was calculated, followed by the TPC. Through Rancimat analysis, the induction times of the samples were measured, and the AAI was determined. The water samples used from the Rancimat analysis were then analyzed for acrolein using the HPLC.

RSA and TPC. The RSA and TPC of the extracts were calculated based on the absorbance values obtained through UV-vis spectrophotometry. The RSA of extracts from *M. calabura* at different concentrations is shown in Table 1.

Table 1. Summary of radical scavenging activity (RSA), and total phenolic content (TPC) of increasing concentrations of leaf extract to DPPH solution. Data used to calculate for RSA and TPC are expressed in average by the UV-vis spectrophotometer.

Concentration (ppm)	RSA (%)	TPC (mg GAE/g)
40-Gallic Acid	94.24	N/A
40	54.59	57.92
80	56.63	60.09
120	60.47	64.16
160	63.47	67.35
200	66.59	69.38

RSA determines how likely the antioxidants present in *M. calabura* prevent the release of free radicals. DPPH is a purple-colored solution that gradually changes to a yellowish solution depending on the presence of antioxidants or antioxidative activity [25]. The absorbance of the gallic acid-DPPH aliquot at 40 ppm was measured to obtain the TPC in terms of mg GAE/g. In DPPH assays with gallic acid as the standard, a TPC value greater than 10 mg GAE/g is considered to have a high antioxidative capability [27]. *M. calabura* leaves are abundant in flavones, isoflavones, and polyphenols, which explain the high values for the TPC [28].

Induction time and AAI. The induction times of the samples were obtained through Rancimat analysis, while the AAI values of the samples were calculated based on the induction times. The induction time of cooking oil is one way to determine oxidative stability. The longer the induction time, the more stable the cooking oil is. The time indicates when the oil starts to break down at a certain temperature, in this case at 150 °C. The AAI explains the relative antioxidative activity between the control and the treated samples; the higher the index, the higher the antioxidant activity of the oil compared to the other [14].

Among the four set-ups, the set-up with 0.5% mass of extract shows the highest induction time and antioxidative index. Both induction time and AAI increased as the percent mass of extract added to PCO increased (0<0.1%<0.3%<0.5%). Meanwhile, the acrolein concentration decreased (0.5%<0.3%<0.1%<0) as shown in Table 2.

Table 2. Summary of mean values for induction time (IT), antioxidative activity index (AAI), and acrolein concentration (AC) of palm cooking oil with increasing percent mass of leaf extract. Data are expressed in terms of mean ± standard deviation (n = 4).

Extract (% Mass)	IT (h)	AAI	AC (ppm)
0	2.30 ± 0.20	1.00 ± 0.00	9.747 ± 0.67
0.1	2.51 ± 0.05	1.10 ± 0.09	8.120 ± 0.22
0.3	2.66 ± 0.06	1.16 ± 0.10	6.914 ± 0.48
0.5	2.78 ± 0.08	1.22 ± 0.08	5.262 ± 0.99

Each treatment group is significantly different (p<0.05) from the control group, which indicates that there is an increase in the oxidative stability of PCO as the mass percent composition of *M. calabura* leaf extract is increased. However, no significant difference (p>0.05) can be found from the pairwise comparisons of the 0.1% and 0.3% set-ups, and the 0.3% and 0.5% set-ups, as reflected in Figure 3.

Acrolein concentrations. To quantify the acrolein concentrations, HPLC analysis was performed on the water samples used for the Rancimat analysis. The acrolein concentrations from cooking oil fumes were observed to decrease as the concentration of extract is increased, as indicated in Table 2. Each pair of set-ups was also significantly different (p<0.05) from one another, as shown by Figure 3. Furthermore, an increase in the percent mass of extract by increments of 0.2% significantly decreased the acrolein

concentrations in the fumes of the oil, unlike the results obtained for induction time.

The approach of analyzing acrolein in PCO fumes through the use of the Rancimat is a novel method that utilizes the concept of polarity and solubility. The volatile oxidation products generated due to the lipid oxidation are directed by the air stream to the Rancimat vessels containing pure water [29]. Since acrolein and water are both polar, acrolein dissolves in water.

Fullana et al. [30] have investigated the level of aldehydes emitted at different times at 180 °C and 240 °C but were unable to analyze acrolein. Aside from their study, no studies have analyzed the aldehyde concentrations in fumes in cooking oil with antioxidant additives but such analysis was recommended [12,18].

The results of Endo et al. [31] show that acrolein in cooking oil is not formed from glycerol backbones in triacylglycerol but from methyl linolenate and methyl linoleate derived from polyunsaturated fatty acids, such as α-linolenic and linoleic acids, produced at high levels during heating. Thus, cooking with vegetable oils at high temperatures is not advisable as it induces the formation of acrolein. Furthermore, Da Silva and Pereira [12] formulated a reaction mechanism on how unsaturated fatty acids degrade to acrolein which provides several unstable singlet oxygens in intermediate reactions accompanied by the production of free radicals along the way. In the nucleophilic attack, antioxidants bind to singlet oxygen molecules to prevent the reduction of carboxylic acids to aldehydes. These antioxidants also bind to the free radicals produced due to oxidation, as shown in Figure 2 [12].

Comparing the values, it can be inferred that the induction time of oil is directly proportional to the antioxidant activity of the oil and inversely proportional to its acrolein emissions. This confirms the proposed association between the amount of natural antioxidants and the aldehyde emissions of the oil [12,18].

The basis for the oxidative stability of cooking oil majorly depends on its polyunsaturated fatty acid composition [32]. Hence, aside from the addition of antioxidants in cooking oil, the mixing of polyunsaturated fatty acid-rich oil with monounsaturated fatty acid-rich oil can be done to increase its oxidative stability [33]. The fatty acid composition of the oil is also the basis in determining the nature of volatile aldehyde formation [30,33]. The four parameters, namely fatty acid composition, antioxidant concentration, induction time, and volatile aldehyde concentration, are likely interrelated and can be the subject of further studies.

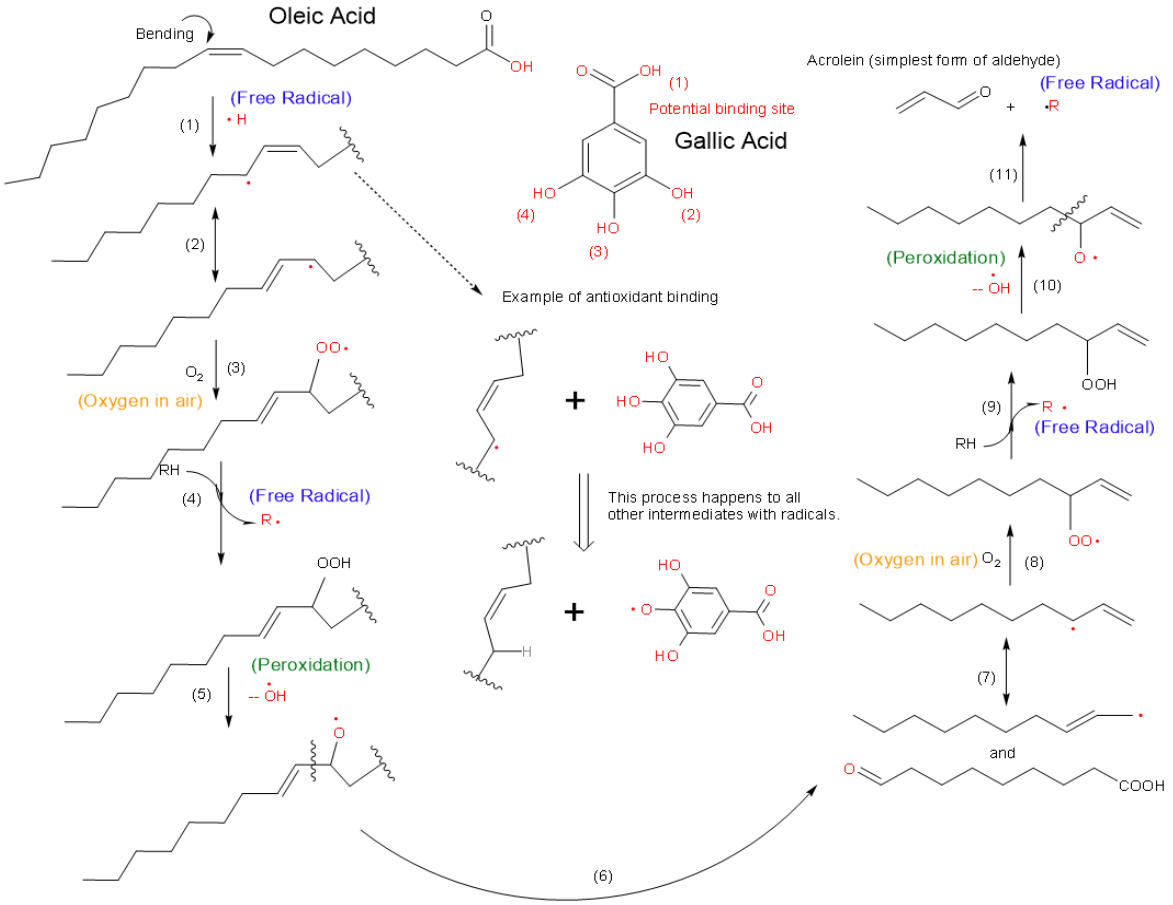

Figure 2. Reaction mechanism of the degradation of oleic acid—a monounsaturated fatty acid in palm cooking oil—into acrolein and the interaction of an antioxidant, gallic acid, in the prevention of such reaction [12].

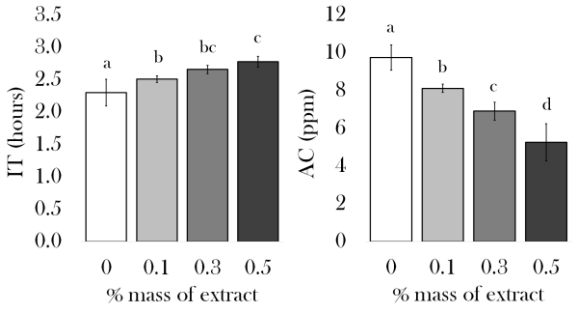

Figure 3. Induction time (IT) and acrolein concentrations (AC) in the fumes of palm cooking oil with varying % mass of *M. calabura* ethanol leaf extract. Data are presented as mean ± standard deviation (n=4). Values with different superscript letters represent significant differences among set-ups (p<0.05).

Limitations. The results of this study partially support the claims in the literature that the addition of antioxidants contributes to the reduction of aldehydes present in cooking oil fumes. However, the researchers were not able to identify specific antioxidants present in the extract. Second, the extract was not freeze-dried to maximize solubility in PCO. Third, the cooking oil used was already incorporated with butylated hydroxytoluene, a synthetic antioxidant. Fourth, other aldehydes aside from acrolein were not analyzed.

Conclusion. - Antioxidant capacity to reduce aldehyde emissions of palm cooking oil was investigated. Before treatment of the oil, it has been verified that *M. calabura* leaves contain high antioxidative activity, total phenolic content, and antioxidative activity index. Induction times of the treated oil samples increased, implying that oxidative stability increased. Hence, the addition of natural antioxidants, specifically *M. calabura* leaf extract, to palm cooking oil increases oxidative stability of the oil and reduces the aldehyde concentrations in palm cooking oil fumes. Significant differences were observed between the induction times of all pairs of set-ups except for the 0.1% and 0.3% pair and the 0.3% and 0.5% pair. Meanwhile, significant differences were observed between the acrolein concentrations of all pairs of set-ups (0 & 0.1%, 0 & 0.3%, 0 & 0.5%, 0.1% & 0.3%, 0.1% & 0.5%, and 0.3% & 0.5%). Lastly, this study can serve as a basis for the establishment of the correlation between the addition of antioxidants in cooking oil and its emission of aldehydes as fumes.

Recommendations. - It is recommended that similar studies are done with the use of gas chromatography-mass spectrometry which is more suited for volatile analytes. Other cooking oils, aldehydes, and sources of natural antioxidants should also be analyzed to compare the power and versatility of the natural antioxidants. Another recommendation is to test the treatments at varying higher temperatures and heating duration. Sensory analysis of the treated oil is also encouraged. Moreover, it is recommended to analyze the fatty acid composition and aldehyde concentrations of oil subjected to high heating temperatures to determine if the results are consistent with the aldehyde emissions. Lastly, antioxidant profiling and the determination of antioxidant binding ability with acrolein could be performed.

Acknowledgment. - The authors would like to extend their gratitude to the Department of Environment and Natural Resources (Region VI) for verifying the species of the plant samples used in the study. Their gratitude is also extended to the Food Science Laboratory of the University of the Philippines Visayas - Regional Research Center for allowing them to perform the Rancimat analysis.

References

[1] Harrison MR, Hester RE, editors. 2019. Indoor air pollution. [Internet]. The Royal Society of Chemistry; [cited 2020 Jan 27]. Available from: https://rsc.li/2lYHDjH.

[2] Chen HC, Wu CF, Chong IW, Wu MT. 2018. Exposure to cooking oil fumes and chronic bronchitis in nonsmoking women aged 40 years and over: a health-care based study. BMC Public Health. 18(246): 1–11. doi: 10.1186/s12889-018-5146-x.

[3] Katragadda HR, Fullana A, Sidhu S, Carbonell-Barrachina AA. 2010. Emissions of volatile aldehydes from heated cooking oils. Food Chem. 120: 59–65. doi: 10.1016/j.foodchem.2009.09.070.

[4] Neghab M, Delikhoon M, Baghani AN, Hassanzadeh J. 2017. Exposure to cooking fumes and acute reversible decrement in lung capacity. Int J Occup Env Med. 8(4):207–216. doi: 10.15171/ijoem.2017.1100.

[5] WHO (World Health Organization). 2018. [Cited 9 September 2019]. Available from https://bit.ly/3ekZASi.

[6] EPA (Environmental Protection Agency). 2019. [Cited 27 January 2020]. Available from https://bit.ly/2SrEuZT.

[7] Rivas I, Fussell J, Kelly F, Querol X. 2019. Indoor Sources of Air Pollutants. Issues Environ Sci Technol. 48: 1–15. doi: 10.1039/9781788016179-00001.

[8] Tham KW. 2016. Indoor air quality and its effects on humans — A review of challenges and developments in the last 30 years. Energy Buildings. 130: 637–650. doi: 10.1016/j.enbuild.2016.08.071.

[9] Haddad M. c2020. Coronavirus: How much more time are people spending at home? [Internet]. Aljazeera Media Network. [cited 2020 December 9]. Available from: https://bit.ly/3h6LHcb.

[10] Ghobadi S, Akhlaghi M, Shams S, Mazloomi SM. 2018. Acid and peroxide values and total polar compounds of frying oils in fast food restaurants of Shiraz, Southern Iran. Int J Nutr Sci. 3(1): 25–30.

[11] Lu F, Shen B, Yuan P, Li S, Sun Y, Mei X. 2019. The emission of PM2.5 in the respiratory zone from Chinese family cooking and its health effects.

Sci Total Env. 654: 671–677. doi: 10.1016/j.scitotenv.2018.10.397.

[12] Da Silva TO, Pereira PA. 2008. Influence of time, surface-to-volume ratio, and heating process (continuous or intermittent) on the emission rates of selected carbonyl compounds during thermal oxidation of palm and soybean oils. J Agric Food Chem. 56(9): 3129–3135. Doi: 10.1021/jf0734525.

[13] Guillaume C, De Alzaa F, Ravetti L. 2018. Evaluation of chemical and physical changes in different commercial oils during heating. Acta Scientific Nutritional Health. 2: 2–11.

[14] Metrohm. 2012. Oxidation stability of oils and fats – Rancimat method. Available from: https://bit.ly/3eYtMBU.

[15] Ali S, Chatha SAS, Ali Q, Hussain AI, Hussain SM, Perveen R. 2016. Oxidative stability of cooking oil blend stabilized with leaf extract of *Eucalyptus citriodora*. Int J Food Prop. 19(7): 1556–1565. doi: 10.1080/10942912.2015.1047514.

[16] Chowdhury K, Banu L, Khan S, Latif A. 2008. Studies on the fatty acid composition of edible oil. Bangladesh J Sci Ind Res. 42(3): 311–316. doi: 10.3329/bjsir.v42i3.669.

[17] Fujisaki M, Endo Y, Fujimoto K. 2002. Retardation of volatile aldehyde formation in the exhaust of frying oil by heating under low oxygen atmospheres. J Amer Oil Chem Soc. 79(9): 909–914. doi: 10.1007/s11746-002-0578-3.

[18] Shahid MZ, Saima H, Yasmin A, Nadeem MT, Imran M, Afzaal M. 2018. Antioxidant capacity of cinnamon extract for palm oil stability. Lipids Health Dis. 17(1): 1–8. doi: 10.1186/s12944-018-0756-y.

[19] Shahidi F, Zhong Y. 2010. Lipid oxidation and improving the oxidative stability. Chem Soc Rev. 39(11): 4067–4079. doi: 10.1039/B922183M.

[20] Taghvaei M, Jafari SM. 2015. Application and stability of natural antioxidants in edible oils in order to substitute synthetic additives. J Food Sci Technol. 52(3): 1272-1282. doi: 10.1007/s13197-013-1080-1.

[21] El-Roby AM, Hammad KSM, Galal SM. 2020. Enhancing oxidative stability of sunflower oil with sesame (*Sesamum indicum*) coat ultrasonic extract rich in polyphenols. J Food Process Preserv. e14564. doi: 10.1111/jfpp.14564.

[22] Recuenco MC, Lacsamana MS, Hurtada WA, Sabularse VC. 2016. Total phenolic and total flavonoid contents of selected fruits in the Philippines. Phil Journal Sci. 145(3): 275–281. doi: 10.1100/2012/728613.

[23] Singh A, Gupta R, Pandey R. 2017. Exogenous application of rutin and gallic acid regulate antioxidants and alleviate reactive oxygen generation in *Oryza sativa L*. Physiol Mol Biol Plants. 23(2): 301–309. doi: 10.1007/s12298-017-0430-2.

[24] Y MAK, Mundasada SC, Ramadas D. 2015. Antioxidative activity: root, leaves and fruits aqueous extracts of *Muntingia calabura*. JIPBS. 2(4): 363–368.

[25] Mohamed S, Mohd NF, inventors; University Putra Malaysia, Selangor, assignee. 2013. Cooking oil composition with additives to reduce oil adsorption. United States Patent Application No. 8.425,969 B2.

[26] Kedare SB, Singh RP. 2011. Genesis and development of DPPH method of antioxidant assay. J Food Sci Technol. 48(4): 412–422. doi: 10.1007/s13197-011-0251-1.

[27] Mahmood ND, Nasir NLM, Rofiee MS, Tohid SFM, Ching SM, Teh LK, Salleh MZ, Zakaria ZA. 2014. *Muntingia calabura*: a review of its traditional uses, chemical properties, and pharmacological observations. Pharm Biol. 52(12): 1598–1623. doi: 10.3109/13880209.2014.908397.

[28] Haerani A, Chaerunisa AY, Subarnas A. 2019. Antioxidant Activities of *Muntingia calabura*, *Syzygium cumini*, *Ocimum basilicum*, and *Eleutherine bulbosa* using DPPH Method. Indonesian Journal of Pharmaceutics. 1(2): 50–54. doi: 10.24198/idjp.v1i2.21531.

[29] Tinello F. Lante A, Bernardi M, Cappiello F, Galgano F, Caruso MC, Favati F. 2018. Comparison of OXITEST and RANCIMAT methods to evaluate the oxidative stability in frying oils. Eur Food Res Technol. 244(4): 747–755. doi: 10.1007/s00217-017-2995-y.

[30] Fullana A, Carbonell-Barrachina AA, Sidhu S. 2004. Comparison of volatile aldehydes present in the cooking fumes of extra virgin olive, olive, and canola oils. J Agric Food Chem. 52(16): 5207–5214. doi: 10.1021/jf035241f.

[31] Endo Y, Hayashi C, Yamanaka, T, Takayose K, Yamaoka M, Tsuno T, Nakajima S. 2013. Linolenic acid as the main source of acrolein formed during heating of vegetable oils. Journal of the American Oil Chemists' Society. 90(7): 959–964. doi: 10.1007/s11746-013-2242-z.

[32] Bhatnagar AS, Prasanth Kumar PK, Hemavathy J, Gopala Krishna AG. 2009. Fatty acid composition, oxidative stability, and radical scavenging activity of vegetable oil blends with coconut oil. J Am Oil Chem Soc. 86(10): 991–999. doi: 10.1007/s11746-009-1435-y.

[33] Maszewska M, Florowska A, Dłużewska E, Wroniak M, Marciniak-Lukasiak K, Zbikowska A. 2018. Oxidative stability of selected edible oils. Molecules. 23(1746): 1–12. doi: 10.3390/molecules23071746.